Techno-economic assessment of the one-step CO_2conversion to dimethyl ether in a membrane-assisted process

Journal of CO2 Utilization 69 (2023) 102419

Contents lists available at ScienceDirect

Journal of CO2 Utilization

journal homepage: www.elsevier.com/locate/jcou

Techno-economic assessment of the one-step CO_2 conversion to dimethyl ether in a membrane-assisted process

Serena Poto [a], Thomas Vink [a], Pierre Oliver [b], Fausto Gallucci [a,c,*], M. Fernanda Neira d'Angelo [a]

[a] Sustainable Process Engineering, Chemical Engineering and Chemistry, Eindhoven University of Technology, De Rondom 70, 5612 AP Eindhoven, the Netherlands
[b] Hydrogen Lab, ENGIE Lab CRIGEN, 4, rue Joséphine Baker, 93240 Stains, France
[c] Eindhoven Institute for Renewable Energy Systems (EIRES), Eindhoven University of Technology, PO Box 513, Eindhoven 5600 MB, the Netherlands

ARTICLE INFO

Keywords:
DME production
Economic analysis
Plant design
Membrane reactors
Process integration

ABSTRACT

This study investigates the impact of the membrane reactor (MR) technology with in-situ removal of water to boost the performance of the one-step DME synthesis via CO_2 hydrogenation at process scale. Given the higher efficiency in converting the feedstock, the membrane reactor allows for a remarkable decrease in the main cost drivers of the process, i.e., the catalyst mass and the H_2 feed flow, by ca. 39% and 64%, respectively. Furthermore, the MR-assisted process requires 46% less utilities than the conventional process, especially in terms of cooling water and refrigerant, with a corresponding decrease in environmental impact (i.e., 25% less CO_2 emissions). Both the conventional and MR-assisted plants were found effective for the mitigation of the CO_2 emissions, avoiding ca. 1.4–1.6 ton_{CO_2}/ton_{DME}. However, given the higher reactor and process efficiency, the membrane technology contributes to a significant reduction (i.e., 25%) in the operating costs, which is a remarkable improvement in this OPEX intensive process. Nevertheless, the calculated minimum DME selling price (i.e., 1739 €/ton and 1960 €/ton for the MR-assisted and the conventional process, respectively) is over 3 times greater than the current DME market price. Yet, with the predicted decrease of renewable H_2 price and a zero-to-negative cost for the CO_2 feedstock, the MR-assisted system could become competitive with the benchmark between 2025 and 2050.

1. Introduction

The anthropogenic CO_2 emissions must be drastically reduced in order to tackle the urgent issue of global warming, which is the top priority challenge of our times [1,2]. In this scenario, the CO_2 capture and storage (CCS) is widely recognized as the most effective way to mitigate the CO_2 concentration in the atmosphere in short term [3]. Nevertheless, processing the captured CO_2 to obtain more valuable products, according to a carbon capture and utilization (CCU) approach, is even more attractive as a long term solution. This would allow, at the same time, to synthesize carbon-based products (e.g., methane, methanol, olefins), reducing our dependency on fossil fuels [4–7]. Among the different products that can be produced from CO_2, dimethyl ether (DME) is very attractive. DME is an alternative clean fuel which can be used in replacement of diesel or LPG with limited changes to the current engines [8,9]. We can identify two distinct DME production routes: 1) the indirect route, where methanol is first produced and then dehydrated in a separate step; 2) the direct route, which is more efficient, where the methanol synthesis and dehydration occur simultaneously in a single reactor [10]. Currently, the feedstock for the methanol production is syngas, which is in turn a product of either steam reforming of natural gas, or gasification of crude oil, coal, or more rarely biomass and municipal solid waste (MSW) [11,12]. Thus, the benchmark DME process is mostly fossil-based and has a CO_2 footprint in the range of 89–98 gCO_2/MJ_{DME} [13–15]. Furthermore, the DME production cost from natural gas was estimated to range between 0.12 and 0.16 USD/kg_{DME} (i.e., a relatively low production cost), as reported by Yoon and Han (2015) [16].

Taking this into account, producing DME from captured CO_2 and renewable H_2 is not only a valid route for CO_2 valorisation and/or H_2 storage [17,18], but also a way to render the process more sustainable [19].

The CO_2 direct (or one-step) hydrogenation to DME can be summarized by the following reaction scheme:

* Corresponding author at: Sustainable Process Engineering, Chemical Engineering and Chemistry, Eindhoven University of Technology, De Rondom 70, 5612 AP, Eindhoven, the Netherlands.
E-mail address: F.Gallucci@tue.nl (F. Gallucci).

https://doi.org/10.1016/j.jcou.2023.102419
Received 5 December 2022; Received in revised form 13 January 2023; Accepted 31 January 2023
Available online 3 February 2023

CO_2 hydrogenation: $CO_2 + 3\ H_2 \rightleftarrows CH_3OH + H_2O\ \Delta H_0 = -49{\cdot}5$ kJ/mol(1)

Reverse water gas shift: $CO_2 + H_2 \rightleftarrows CO + H_2O\ \Delta H_0 = +41{\cdot}2$ kJ/mol (2)

Methanol dehydration: $2CH_3OH \rightleftarrows CH_3OCH_3 + H_2O\ \Delta H_0 = -23{\cdot}4$ kJ/mol (3)

The overall process is exothermic and is thermodynamically favoured by high pressures and low temperatures. Both the methanol synthesis (1) and the reverse water gas shift (r-WGS) reaction (2) are carried out over a Cu-ZnO-Al_2O_3 catalyst [20,21] although novel catalyst formulations to improve the CO_2 activity have been proposed in the last few years [22–24] On the other hand, the methanol dehydration reaction (3) requires acid catalysis, which is often given by materials such as γ-Al_2O_3, silico-aluminates and zeolites (e.g., HZSM-5, FER, MOR.) [25,26] As a result, the one-step DME synthesis requires a bi-functional catalyst, which normally is a physical mixture of the methanol synthesis and dehydration catalyst. All the reactions (1–3) lead to the formation of large volumes of water as a by-product, which contributes to the strong thermodynamic limitations of the system, as well as to catalyst deactivation in long term operation [27–29]. Thus this process would enormously benefit from the in-situ removal of water from the reaction environment.

The integration of water selective membranes in a so-called membrane reactor (MR) has proved to be an effective strategy to overcome the thermodynamic limitations in the DME synthesis [9,30–33]. In our recent study, we demonstrated that removal of ca. 96% of the water produced leads to an improvement of the CO_2 conversion and DME yield of 36% and 46%, respectively [34]. We proposed a fixed bed membrane reactor configuration with a co-current circulation of a sweep gas containing the reactants (i.e., CO_2 and H_2), and studied the effect of the reaction conditions based on ideal membrane properties. To the best of our knowledge, only two studies have investigated the integration of the membrane reactor technology for the DME synthesis at flowsheet level. De Falco et al. [35] introduced a specific plant architecture named "Double Recycling Loop DME production" (DRL-DME), which is based on the simultaneous recycle of the CO_2 streams from the permeation zone and the unconverted gas from the reaction zone. In this study, the authors proposed the use of zeolite membranes to promote the water separation, using a CO_2 rich syngas as feedstock. More recently, Hamedi et al. [36] proposed a comparison of the conventional (i.e., with packed beds) direct DME synthesis via CO_2 hydrogenation route with its MR-assisted counterpart, based on an energy assessment of the two technologies. The authors found that the MR technology allows for a reduction of the heating and refrigerant demands of ca. 44.5% and 69.4%, respectively. Nevertheless, neither of these studies has investigated the economics of the two process configurations and, especially the impact of the MR technology on both capital investment and operating costs. As a matter of fact, some researchers have already identified the cost of hydrogen as the main bottleneck of any CO_2 hydrogenation process [19,37–39] which is the main factor that currently holds back industries from investing in these technologies.

Therefore, this study proposes a comparison on a techno-economic level of two routes for the one-step DME synthesis via CO_2 hydrogenation: 1) the conventional route, based on a packed bed reactor (PBR) technology; and 2) the MR-assisted route, based on the packed bed membrane reactor technology (PBMR). The two processes are designed at relatively large scale (i.e., 10 kton/y of DME), and optimized with the objective of minimizing the energy requirement and the H_2 consumption; as well as maximizing the efficiency at both reactor and process scale, reducing as much as possible the utilities consumptions. The main goal is to assess whether the membrane reactor technology can significantly improve the performance at process scale, and therefore increase the industrial attractiveness of this CO_2 valorisation route. Furthermore, we propose a detailed analysis of the possible conditions which could render our technology more competitive with the DME market price in the future. We consider different routes for the H_2 production, as well as different scenarios regarding the price of the CO_2 feedstock based on the relationship between the carbon capture cost and the carbon tax. Finally, based on these scenarios and on cost predictions, we aim at identifying the moment in which this technology will be industrially appealing and the factors which could delay/anticipate its applicability at large scale.

2. Methodology and assumptions

Mass and energy balance calculations were carried out via process flow modeling using Aspen Plus V11 and MATLAB R2019a software. Process intensification strategies (i.e., the use of membrane reactors), and heat integration were proposed as a way to improve the energy efficiency of the process. Afterwards, the impact of the capital investment (CAPEX) and operational cost (OPEX) on the minimum DME selling price (MDSP) necessary to make the system profitable was assessed.

2.1. System boundaries

- This analysis focuses on the DME production while the CO_2 capture, purification and transport, as well as the H_2 generation and transport are out of the scope of this work. As a base case, we assumed that CO_2 is obtained via sorption enhanced water gas shift (SEWGS) process from iron and steel off-gases [40], while H_2 is assumed to be supplied by an integrated pipeline network and produced via a range of the most cost efficient technologies, as determined by the JRC-EU-TIMES model [39,41]. The H_2 production technologies identified by this model are mostly based on steam methane reforming, coal and biomass gasification, coupled with the CCS. Next, we propose a sensitivity analysis on the cost of H_2 and CO_2 to evaluate different alternatives as well as to consider sustainable production methods, in strive for a lower carbon footprint of the entire supply chain. The H_2 and CO_2 streams are assumed to enter the plant at 3.5 MPa and 25 °C, and ambient conditions, respectively. The purity of both streams entering the plant is assumed 100%, since the purification of such streams generally take place at the site of generation. This assumption is stronger for the CO_2 stream, where the purification can significantly affect its cost. However, the effect of the purification is incorporated in the sensitivity analysis on the feedstock price.
- The DME production process comprises the following sections: 1) two multistage compression sections for the H_2 and CO_2, respectively, 2) DME synthesis reactor via one-step CO_2 hydrogenation in either PBRs or PBMRs, 3) DME purification via condensation and distillation train, 4) recycle of unconverted gas and recovery of by-product; and 5) the heat exchanger network. All these sections constitute the plant inside battery limits (ISBL). The outside battery limits (OSBL) comprises: 1) the HP-steam generation system, 2) a cooling tower and 3) a refrigeration cycle based on propylene. The electricity is assumed to be derived from the grid.
- Both plants target a DME productivity of 10 kton/ year (kTA). Typical methanol production plants have productivity ranging from 0.03 to 800 kTA [42]. Being methanol the conventional feedstock for the DME production ($2CH_3OH \rightleftharpoons CH_3OCH_3 + H_2O$), the proposed plant size falls in the range of typical industrial scale plants. Furthermore, we assume a plant lifetime of 20 years, with a production time of 8000 h per year, which corresponds to a capacity factor of 91.3% [39].
- Both technologies are designed to obtain DME *fuel* grade, according to the specification given by the ISO16861 normative developed in 2015 [43].

- The plant is considered to be built in The Netherlands, where the average temperature is 11 °C and can go up to 19.5 °C during summer, with an average humidity of 79% [44]. The current carbon tax in the Netherlands is above average when compared to the rest of Europe [45], making our study more conservative on this aspect. Thus, we propose a sensitivity analysis also on this parameter to evaluate different scenarios and to reflect various geopolitical situations.

2.2. Basis and assumptions for reactor design and sizing

- The packed bed reactor (PBR) and packed bed membrane reactor (PBMR) design is based on a 1D pseudo-homogeneous plug flow reactor model, assuming a unitary catalyst effectiveness (i.e., no internal diffusion limitations), no external mass transfer limitation, and no temperature gradients at the particle scale as well as in the reactor radial direction.
- The reactor model consists of mass and energy balances, coupled with the Ergun equation for the estimation of the pressure drops in the catalytic bed. Details on the model equations are reported in the supplementary information (S.I.).
- The catalytic bed includes a bifunctional catalyst based on a physical mixture of 90 wt% $Cu/ZnO/Al_2O_3$ for the methanol synthesis and 10 wt% of HZSM-5 for the methanol dehydration, which follows the kinetics proposed by Portha et al. [46] and Ortega et al. [47], respectively. The reaction kinetics was considered to be unaffected by the presence of the membranes. Details on the reaction pathway and kinetics are reported in S. I., together with the experimental validation and optimization of the composition of the catalytic bed (i.e., mass ratio of the $Cu/ZnO/Al_2O_3$ and HZSM-5). To prevent hot spots, silicon carbide (SiC) is added to the catalyst bed with a volumetric dilution factor of 2/3. An average particle size (d_p) of 3 mm was assumed for both catalyst and diluent. The solid hold-up (ε_s) is set to 0.6 $m^3_{solid}/m^3_{reactor}$.
- A H_2:CO_2 stoichiometric ratio of 3, and a total pressure of 40 bar, based on our previous work [34].
- Circulating boiling water in an external reactor shell was selected as heat management solution to guarantee a nearly isothermal operation. Therefore, the temperature of the boiling water (T_w) was optimized accordingly. The flow rate of the boiling water ($\dot{m}_w$) was determined in such a way that the heat removed from the reaction environment could be used for the production of medium pressure (MP) steam (i.e., latent heat exchange).
- The membrane module of the PBMR consists of tubular ceramic-supported carbon molecular sieve membranes (CMSMs), which show promising performance in terms of vapor/gas separation and stability in hot and humid environment, according to our previous work [48]. The properties of the membranes in terms of permeance of H_2O, H_2, CO_2, CO and CH_3OH as a function of temperature were determined experimentally and fitted with an Arrhenius law [49] (details in S.I.). DME permeance was assumed to be 50 times lower than that of H_2O [50]. A relatively low gradient in total pressure (ΔP = 5 bar) between the reaction and permeation zone was selected to ensure the selective removal of water and, at the same time, to retain the reactants in the reaction zone. To the same scope, the reactants (i.e., CO_2, H_2 with H_2:CO_2 of 3) are circulated in the permeation zone as a sweep gas [34]. The *SW* ratio, defined as the ratio between the flow rate of the sweep gas and the feed flow rate, is another parameter regulating the driving force for the water removal. In a previous study, we proposed an optimal value for *SW* of 20 to remove effectively both the water and the heat from the reaction environment. However, this would require an excessive H_2 make-up for the sweep gas recirculation, which has been identified as the most critical cost driver of the CO_2 hydrogenation processes [19,39]. Thus, this works assumes a *SW* of 1 to reduce H_2 consumption, while the heat management of the PBMR also relies on the circulation of boiling water in an external mantle.
- The reactor operating conditions (i.e., temperature and GHSV) were first optimized for the PBR. Thereafter, the PBMR was assumed to operate in the same conditions and a sensitivity analysis was carried out to determine the optimal normalized membrane area (NA_m), as defined in Eq. 4, as well as the composition of the sweep gas in terms of methanol molar fraction.

$$NA_m = \frac{A_m}{\Phi^R_{in}} \tag{4}$$

- The PBR and PBMR were sized to meet the target plant productivity, accounting for the DME recovery in the separation section. The length and diameter of the reactors were determined assuming an aspect ratio (L/D) of 5. The maximum reactor length was set to keep the average temperature equal to the optimal value without the need to increase the boiling water flow. As a result, the number of parallel reaction units was calculated. The reactor shell (or cooling mantle) diameter for the circulation of boiling water was designed assuming a maximum pressure drops of 0.5 bar [51].

2.3. Basis and assumptions for process modelling

- The flash drums design was based on sensitivity analyses to determine the temperature and pressure necessary to achieve a 95% recovery of DME in the liquid phase. A 95% approach to the thermodynamic equilibrium was assumed.
- The distillation columns design and optimization was carried out using the DTSW and RadFrac models in Aspen Plus. The number of stages (N), reflux ratio (R), feed position and the distillate-to-feed ratio (D/F) were first estimated via the DSTW and later optimized by means of a more rigorous model (RadFrac), which allows to determine the mass and energy balance of the system. We assumed a pressure drop per-stage of 7 mbar [52], a Murphee efficiency of 85% to account for deviation from the equilibrium. Column internals are trayed and the column diameter, tray spacing and hole area/active area ratio were optimized to avoid drying up and with a 80% approach to flooding.
- The heat exchanger network (HEN) was designed based on the pinch analysis [53]. Counter-current shell and tube heat exchangers were modeled in Aspen Plus, using a shortcut method on design basis. A minimum temperature difference (ΔT_{min}) of 5 °C was assumed for mild temperature conditions. For temperatures below 0 °C and above 200 °C, the ΔT_{min} was increased to 10 °C.
- All the turbomachines (compressors, pumps and steam turbines) were modeled in Aspen Plus assuming an isentropic and a mechanical efficiency to determine the thermodynamic conditions of the outlet stream and the energy balance. The isentropic and mechanical efficiency was assumed to be 0.85 and 0.95 for compressors and pumps, respectively. For the MP-steam turbine, an isentropic and mechanical efficiency of 0.8 and 0.99 are assumed, respectively [54].
- HP steam at 40 bar and 250 °C is produced pressurizing and vaporizing the waste water stream from the separation train. The required heat duty for the boiler is generated by the combustion of natural gas in a furnace. The combustion temperature was set at 1100 °C and the flow of air was determined by

assuming a concentration of O_2 in the exhaust of 4 vol%, to ensure complete combustion. The net thermal efficiency of the industrial boiler was set at 90% [55].

- A cooling tower is used to reduce the costs of the cold utilities via the recirculation of the cooling water in the system. The required air flow as well as the amount of water which evaporates were calculated assuming a relative humidity of the air of 79% and an average air temperature of 20 °C, to design the tower in the worst-case scenario. The cooling water outlet temperature from the tower was set at 25 °C. The make-up of fresh water that needs to be fed to the system corresponds at least to the amount of water that evaporates in the cooling tower.

2.4. Basis and assumption for the economic analysis and economic indicators

The CAPEX was estimated via the factorial method based on Lang factors, according to which the CAPEX is a factor of the purchase equipment cost (PEC), as reported in Table 1 [56–58].

For the calculation of the PEC, correlations from W. D. Seider [59] and R. Smith [60] were used, based on 2000 and 2002 as reference year, respectively. The PEC is then actualized to the base year of this study (i.e., 2020) using the Chemical Equipment (CE) index, as reported in Eq. 5, where C_P is the purchase cost of equipment.

$$PEC = C_P \frac{CE_{2020}}{CE_{ref}} \quad (5)$$

Details on the correlations used for the calculation of the purchase equipment cost of all the equipment are reported in SI.

The OPEX is defined as the sum of the variable and fixed operating costs $OPEX_{variable}$ and $OPEX_{fixed}$, respectively. The $OPEX_{variable}$ depends on the cost of the feedstock (i.e., CO_2 and H_2), utilities (i.e., electricity, cooling water, natural gas), the waste water treatment and the annualized cost for the catalyst and membranes, for which a lifetime of 2 and 5 years was assumed, respectively [19,61]. The values used for these costs are reported in Table 2.

The $OPEX_{fixed}$ are calculated on an annual basis and the methodology adopted for their estimation is summarized in Table 3. The labor requirement is calculated based on the number of operators required on site and on the average yearly salary in the Netherlands (i.e., 55,000 € [65]), as reported in SI.

To compare the impact of CAPEX and OPEX and to evaluate the total annual cost (TAC), the CAPEX is calculated on an annual basis (ACAPEX), according to the methodology reported in SI. The total annual cost (TAC) is determined via Eq. 6, as follows:

$$TAC = OPEX + ACAPEX \quad (6)$$

The minimum DME selling price (MDSP) or levelized cost of the DME produced was determined based on the discounted cash flow (DCF) analysis, reported in SI. All the financial parameters and assumptions required for the calculation of the ACAPEX and the MDSP are reported in Table 4. The plant is assumed to be financed in a 50/50 debt/equity split. Considering a 4% interest rate on debt according to the recent interest rate charges [66], and a cost of equity of 12%. The capital investment is assumed to be spent in a three-year construction period as follows: 20%, 50% and 30% for each consecutive year. The price of raw materials, utilities, product and by-products are estimated for the year 2020 and are considered constant for the next 20 years, as a base case. The best method of depreciation was evaluated within the analysis, based on the expected cash flow for the generic year *n*. The plant is expected to be fully depreciated at the end of its life, so no salvage value is expected.

Table 1
CAPEX estimation methodology via factorial method based on Lang factors [56,57].

Cost component	**Lang factor**
Purchase Equipment Cost (PEC)	1
Purchase equipment installation	0.39
Instrumentation and controls	0.26
Piping	0.31
Electrical system	0.1
Building (including services)	0.29
Yard improvements	0.12
ISBL	**2.47 · PEC**
OSBL	**0.12 · ISBL**
Engineering and supervision	0.32 · (ISBL+OSBL)
Construction expenses	0.34 · (ISBL+OSBL)
Legal expenses	0.04 · (ISBL+OSBL)
Contractor's fee	0.19 · (ISBL+OSBL)
Indirect Costs (IC)	**0.89 · (ISBL+OSBL)**
Project contingency	0.15 · (ISBL+OSBL+IC)
Process contingency	0.05 · (ISBL+OSBL+IC)
Fixed Capital Investment (FCI)	**1.2 · (ISBL+OSBL+IC)**
Working Capital (WC)	0.15 · FCI
Start-up costs	0.06 · FCI
CAPEX	**1.21 · FCI**

Table 2
Prices assumed for the variable operating costs ($OPEX_{variable}$).

Cost voice	Price	Unit	Reference
H_2 (integrated pipeline network)	2945	€/ton	[39,62]
CO_2 (SEWGS)	33	€/ton	[40]
Electricity	0.06	€/kWh	[63]
Cooling water	0.2	€/ton	[59]
Waste water treatment	0.4	€/ton	[39]
$CuO/ZnO/Al_2O_3$	95.2	€/kg	[39]
HZSM-5	22	€/kg	[19]
Natural gas	0.036	€/kWh	[63]
Al-supported carbon Membrane	1950	€/m^2	[61]
Methanol[a]	390	€/ton	[64]

[a] The price of methanol was used to determine the selling price of the methanol as a by-product

Table 3
Methodology for the estimation of the $OPEX_{fixed}$.

Cost component	Value
Supervision	0.25 · Labor
Direct overhead	0.25 · (Labor + Supervision)
General overhead	0.65 · (Labor + Supervision + Direct overhead)
Maintenance labor	0.65 · FCI
Maintenance materials	0.03 · ISBL
Insurance and tax	0.015 · FCI
Financing working capital	Debt interest · WC

Table 4
Financial parameters and assumptions.

Parameter	Value
Location	Netherlands
Base year	2020
Project lifetime (y)	20
Construction period (y)	3
Plant availability (h/y)	8000
Tax rate (%)	25
Equity/Debt rate	50/50
Debt interest rate (%)	4
Cost of equity (%)	12
WACC (%)	8
Depreciation period (y)	10
Salvage value (€)	0
Exchange rate (USD/EUR)	1.142

2.5. Technical and environmental key performance indicators (KPIs)

The definitions of the CO_2 conversion and DME yield at both reactor (i.e., per-pass) and process scale (i.e., taking into account the recycle streams) are reported in Eqs. 7–10. In the performance evaluated at reactor scale, the subscript R and P stand for either reaction and permeation zone, respectively. The loss or cofeeding of CO_2 (i.e., through back-permeation of sweep gas in the reaction zone) was considered in the terms $F_{CO_2,tmb}$ and $F^*_{CO_2,tmb}$ [34]. Another important KPI of the membrane reactor is the efficiency of the water removal (*WR*, Eq. 11), which represents how effectively the membrane removes the water produced by the reaction system. This last indicator can be derived for each species permeating through the membrane.

$$(X_{CO_2})_{per-pass} = \frac{F^R_{CO_2,0} - F^R_{CO_2} + F_{CO_2,tmb}}{F^R_{CO_2,0} + F^*_{CO_2,tmb}} \tag{7}$$

$$(Y_{DME})_{per-pass} = \frac{2\left(F^R_{DME} + F^P_{DME}\right)}{F^R_{CO_2,0} + F^*_{CO_2,tmb}} \tag{8}$$

$$(X_{CO_2})_{process} = \frac{F^{in}_{CO_2} - F^{out}_{CO_2}}{F^{in}_{CO_2}} \tag{9}$$

$$(Y_{DME})_{process} = \frac{2F^{out}_{DME}}{F^{in}_{CO_2}} \tag{10}$$

$$WR = \frac{F^P_{H_2O}}{F^P_{H_2O} + F^R_{H_2O}} \tag{11}$$

The plant performance was then evaluated in terms of efficiency indexes, as described below.

The cold gas efficiency (CGE, Eq. 12), defined as the ratio of the energy content of the valuable products (i.e., DME and methanol) and the energy content of the feed (i.e., H_2), where the energy content refers to the low heating value (LHV).

$$CGE = \frac{\dot{m}_{DME} LHV_{DME} + \dot{m}_{MeOH} LHV_{MeOH}}{\dot{m}_{H_2} LHV_{H_2}} \tag{12}$$

A low H_2 consumption reflects a high potential for the commercialization of the process. As a result, we defined (Eq. 13) an index representing the H_2 consumption per unit of hydrogenation product (η_{H_2toDME}). The η_{H_2toDME} can assume a minimum value of 0.26 ton/ton, which corresponds to a complete conversion of H_2 to DME.

$$\eta_{H_2toDME} = \frac{\dot{m}_{H_2}}{\dot{m}_{DME}} \tag{13}$$

The definition of the overall plant efficiency (η_{tot}) was re-adapted from previous works [54,67], as follows (Eq. 14).

$$\eta_{tot} = \frac{W_{chem}}{W_{feed} + W_{NG} + \frac{W_{El,in \leftrightarrow out}}{\eta_{El}}} \tag{14}$$

The chemical energy (W_{chem}) and the energy of the feed (W_{feed}) correspond to the energy content of the product and of the H_2, respectively, defined in terms of LHV, as in Eq. 12. The denominator of η_{tot} represents the energy input to our system, necessary for the production of the chemical energy (W_{chem}) contained in the products. As a result, besides the energy corresponding to the H_2 (W_{feed}), we need to account for the energy of the natural gas (W_{NG}) necessary for the production of the HP-steam and the net electricity consumed/produced ($W_{El,in \leftrightarrow out}$). Since we did not account for the production of electricity in our process, we assumed that electricity is produced with a natural gas combined cycle, with a net efficiency (η_{El}) of 58.4% [54].

Next, the level of heat integration of the process is assessed with the efficiency of the utilities ($Z_{utilities}$), which represents the amount of cooling (i.e., propylene used as refrigerant and cooling water) and heating (i.e., HP-steam) utilities compared to the amount of DME produced (Eq. 15(12)).

$$Z_{utilities} = \frac{F_{propyl.} + F_{CW} + F_{steam}}{F_{DME}} \tag{15}$$

where $F_{propyl.}$, F_{CW} and F_{steam} are the molar flow rate of propylene, cooling water and steam and F_{DME} is the molar flow of DME produced by the industrial plant.

The carbon footprint of the produced DME was evaluated in terms of net CO_2 emissions ($\dot{m}_{CO_2,emissions}$), and CO_2 avoided or used ($\dot{m}_{CO_2,avoided}$), as in Eqs. 16 and 17. The direct CO_2 emissions ($\dot{m}_{CO_2,direct}$) include both the unconverted CO_2 which is not recycled (i.e., purge streams), and the CO_2 produced after the combustion of the natural gas for the HP steam generation. The second term of Eq. 16 ($W_{El,in} \bullet \dot{m}_{CO_2,CC}$) represents the indirect CO_2 emissions related to the production of the electricity, assumed on average as 330 g_{CO_2}/kWh as in a natural gas combined cycle [68]. The indirect fraction of $\dot{m}_{CO_2,emissions}$ only accounts for the generation of the utilities. The CO_2 emissions related to the feedstock (i.e., H_2 production, CO_2 capture, as well as their storage and transport) are neglected, being a thoroughly life cycle assessment out of the scope of this work.

$$\dot{m}_{CO_2,emissions} = \sum \dot{m}_{CO_2,direct} + W_{El,in} \bullet \dot{m}_{CO_2,CC} \tag{16}$$

$$\dot{m}_{CO_2,avoided} = \dot{m}_{CO_2,in} - \dot{m}_{CO_2,emissions} \tag{17}$$

3. Process modelling results

3.1. Conventional DME production process

3.1.1. Packed bed reactor design

Fig. 1 evaluates the effect of the reaction temperature and GHSV under isothermal conditions on the conversions and yields. Given the exothermicity of the desired reactions, temperature has a negative effect on DME yield (Y_{DME}) and CO_2 conversion (X_{CO_2}) in favor of the CO yield (Y_{CO}), as depicted in Fig. 1**a**. Indeed, being the r-WGS reaction (reaction 2) endothermic, an increase in the reaction temperature favors the production of CO. On the other hand, the catalyst requirements to reach the optimal gas hourly space velocity (GHSV) decrease exponentially with temperature (i.e., the catalyst mass decreases by 82% from 200 to 220 °C), while the change in DME yield is almost linear. As a result, a reaction temperature of 220 °C was selected as a trade-off. The optimal GHSV which maximizes Y_{DME} at these conditions is 64.3 h^{-1} (Fig. 1**b**), which is comparable to the range of space velocities reported in literature for similar systems [19]. A boiling water temperature (T_w) of 196 °C and a corresponding pressure of 14.3 bar was found optimal, keeping an average temperature of 220 °C. Based on these results, the reactor was sized to meet the target DME productivity. Size characteristics and operating conditions of the reaction unit of the conventional DME production process are summarized in Table 5. Pressure drops were found negligible (ca. 0.025 bar), given the low gas superficial velocity and the large catalyst particle size.

3.1.2. Conventional process description

Fig. 2 depicts the process flow diagram of the one-step CO_2 conversion to DME using conventional packed bed reactors. CO_2 enters the plant at ambient conditions (i.e., 1 bar and 25 °C) as stream 28 and it is compressed to 40 bar (i.e., working pressure of the PBR reactor units) via a multistage compressor unit (MCU) comprised of four compressors (C1 to C4) with intermediate cooling. The outlet temperature of each heat exchanger of the MCU is ca. 35 °C. Then, H_2 is fed to the system at 35 bar and 25 °C (stream 36), and it is compressed to 40 bar via a single stage compressor (C6). The pressurized H_2 and CO_2 feed streams (stream 38) mix with the recycle (stream 23), and the resulting stream (stream 25) is first pre-heated to 195 °C in E1 using the heat of the effluent gas

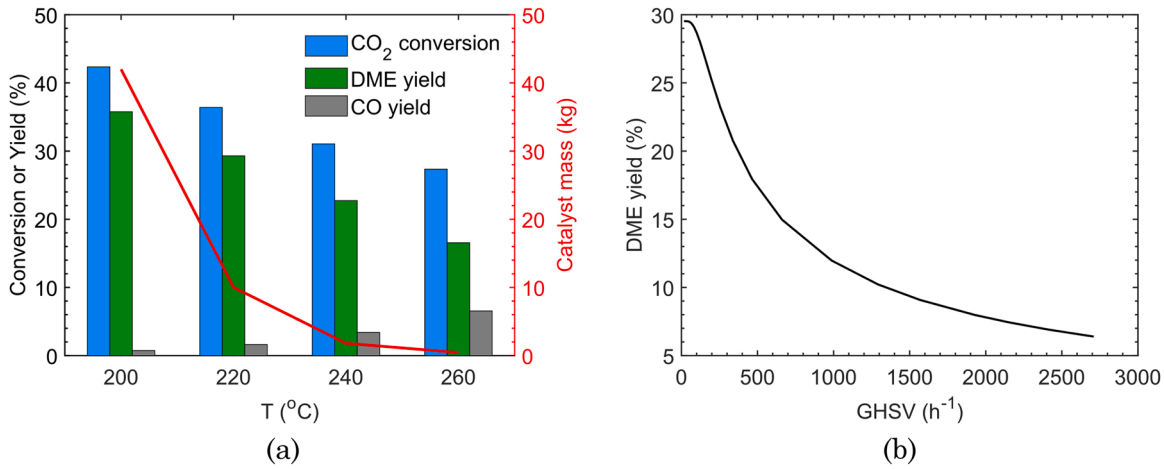

Fig. 1. CO_2 conversion, DME yield and CO yield (left side bars) and on the catalyst mass (right side line) as a function of temperature (a) and DME yield as a function of the GHSV at 220 °C (b).

Table 5
Characteristics of the PBR-based reaction section in terms of size of reactors, number of reactors, catalyst bed properties and operating conditions. The inlet catalyst mass, the inlet volumetric flow and the boiling water mass flow are reported as the sum of the two PBR.

Geometrical properties of the PBR section			
Parameter	**Value**		
Number of reaction units	2		
Reactor length (L)	16.1 m		
Reactor ID (D_{ri})	3.22 m		
Reactor OD (D_{ro})	3.38 m		
Reactor shell ID (D_{si})	3.5 m		
Reactor shell OD (D_{so})	3.55 m		
Parameter	**Value**	**Parameter**	**Value**
Total catalyst mass (m_{cat})	126.2 ton	CuZA/HZSM-5 mass ratio	9 kg/kg
Inlet pressure (P_{in})	40 bar	Inlet temperature (T_{in})	200 °C
Catalyst particle size (d_p)	3 mm	Bed porosity (ε)	0.4 $m^3_{void}/m^3_{reactor}$
Space velocity ($GHSV$)	64.3 h^{-1}	Catalyst dilution	1.33 kg_{SiC}/kg_{cat}
H_2:CO_2 feed molar ratio	3 mol/mol	Inlet volumetric flow (Φ_{in})	16,871 Nm^3/h
BW mass flow ($\dot{m}_w$)	2.14 ton/h	BW temperature (T_w)	196 °C

from the reaction section, and then to 200 °C (i.e., reactor inlet temperature) in E13 using HP steam. Once conditioned, the gas stream (stream 27) is fed to the reaction section, which comprises two parallel PBRs working at average temperature of 220 °C and pressure of 40 bar. The outlet stream from the reaction zone (stream 0) is then re-compressed to 40 bar to overcome the pressure drops encountered in the reactors (i.e., 0.025 MPa) prior to the recycle. This also allows a high DME recovery ($\geq$ 95%) in the condensation step, which, given the high volatility of DME, takes place in the flash drum V1 at − 33.4 °C. To minimize the cooling requirements, this is done in five consecutive heat exchangers (i.e., E1-E5) that allow integration of the heat generated in the reaction in other parts of the process, namely the pre-heating of the inlet stream to the reactor (E1) and heating of the liquid produced at the flash drum V1 (E2). The remaining heat is used to heat up cold utilities (i.e., cooling water for E3 and E4 and propylene for E5). The flash drum V1, separates a vapor phase containing CO, H_2 and part of the CO_2 at the top (stream 8), from a liquid phase stream containing DME, methanol, water and a large portion (i.e., CO_2 mass fraction of 44.1%) of CO_2 at the bottom (stream 7). The gaseous stream (stream 8), together with the CO_2 separated within the distillation train (stream 13), is recycled back to the reactor, with a recycle ratio of 99% (i.e., 1% of the stream is purged as gas waste). The liquid stream from V1 (stream 7)., instead, is first heated to 90 °C (E2) and fed to the first distillation tower (T1). The distillation tower T1 operates at 40 bar in a temperature range of 64.7 °C-235.4 °C to separate DME and CO_2 over the top (stream 10) and methanol and water at the bottom (stream 11). The DME/CO_2 stream is cooled down to 45 °C (E6) and fed to the column T2, operating at 40 bar and 4.8 °C-110.6 °C, to separate CO_2 at the top (stream 13) and to produce a *fuel* grade DME (i.e., purity of 99.91 wt%) at the bottom (stream 15). The pure DME stream is then depressurized to 10 bar and cooled down to 35 °C (E11), which are the typical DME liquid storage conditions. Finally, stream 11, bottom product of T1, is depressurized to 30 bar and fed to the last distillation tower (T3), which operates in a temperature range of 185–234 °C, to separate 99.92 wt% pure water at the bottom (stream 21) and industrial grade methanol at the top (stream 18), which is then depressurized to 10 bar and cooled down to 35 °C (E10). Details on the mass balance of the plant (i.e., stream tables) are reported in S.I. The generation and usage of the utilities are also reported in the scheme in Fig. 2 with dotted lines.

3.2. MR-assisted DME production process

3.2.1. Packed bed membrane reactor design

The packed bed membrane reactor was designed according to the procedure described in Section 2. The operating pressure and temperature of the reaction zone are the same as those identified for the conventional packed bed reactor, while, the conditions regulating the driving force across the membrane (i.e., ΔP and SW) were selected from our previous study [34]. To prevent any loss of reactant (especially the costly H_2) across the membrane, a sweep gas with a similar composition and pressure as those in the feed stream is fed to the permeation zone. An extensive discussion on this configuration is given in our previous work [34]. Nevertheless, this strategy alone is not effective to prevent methanol removal (MR), which can achieve values above 50% (Fig. 3a, right axes), resulting in an increase in Y_{MeOH} and a decrease in Y_{DME}, lowering the efficiency of the membrane reactor. A sensitivity analysis was carried out to determine the normalized membrane area (NA_m) that maximizes Y_{DME} (Fig. 3a). The Y_{DME} displays an optimum corresponding to NA_m of ca. $3.65{\cdot}10^{-2}$ $m^2{\cdot}h/Nm^3$. Greater membrane areas lead to a decrease in Y_{DME} due to the removal of methanol from the reaction zone. Alternatively, the concentration of methanol in the sweep gas can also be optimized to prevent losses. Therefore, we optimized the methanol concentration in the sweep gas to keep the Y_{MeOH} close to zero, which means that all the methanol produced is effectively converted to DME and does not permeate through the membrane. We found that a molar fraction of methanol of 6.37%, together with a normalized membrane

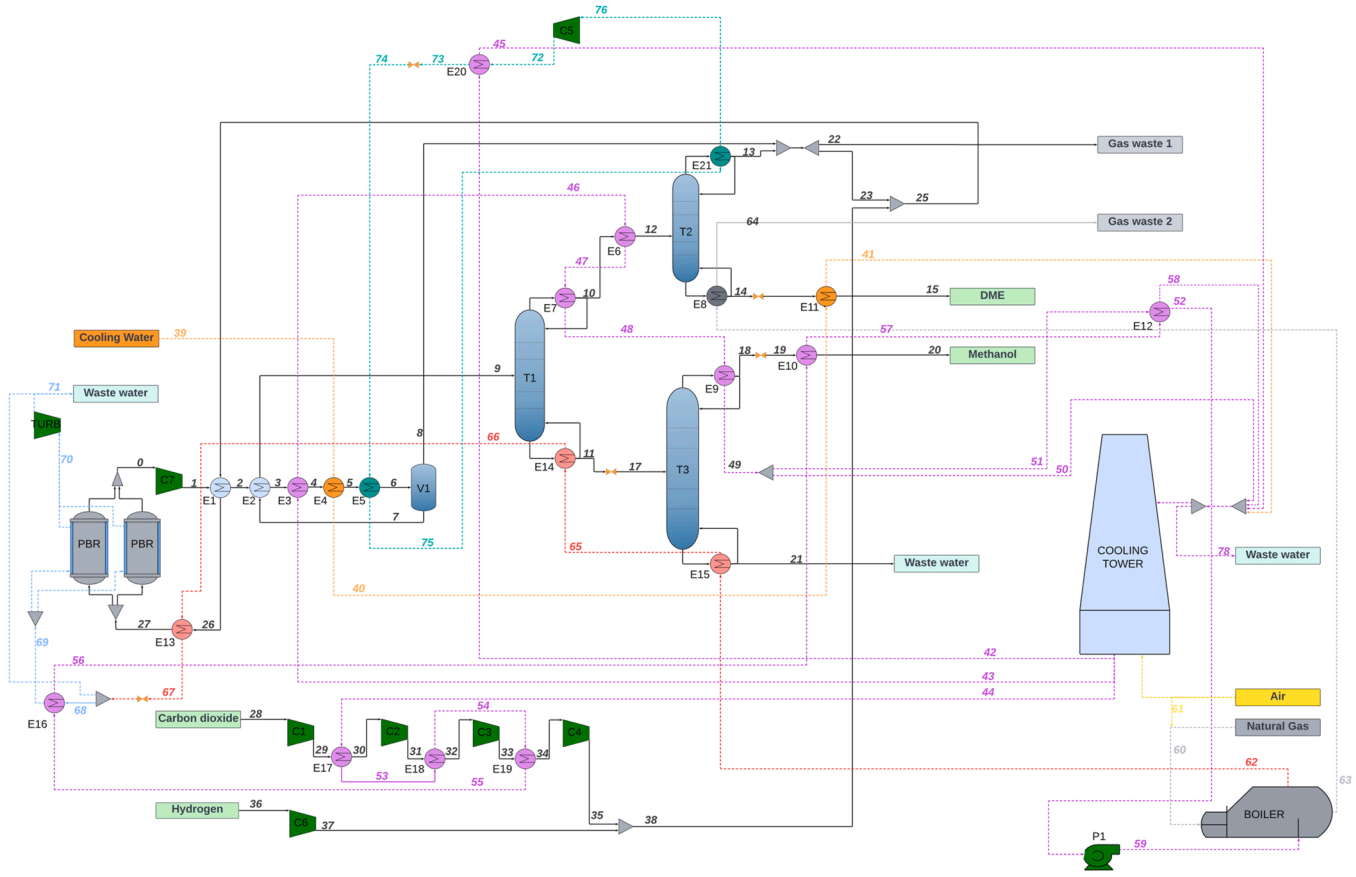

Fig. 2. Process flow diagram of the one-step CO_2 conversion to DME process via packed bed reactors.

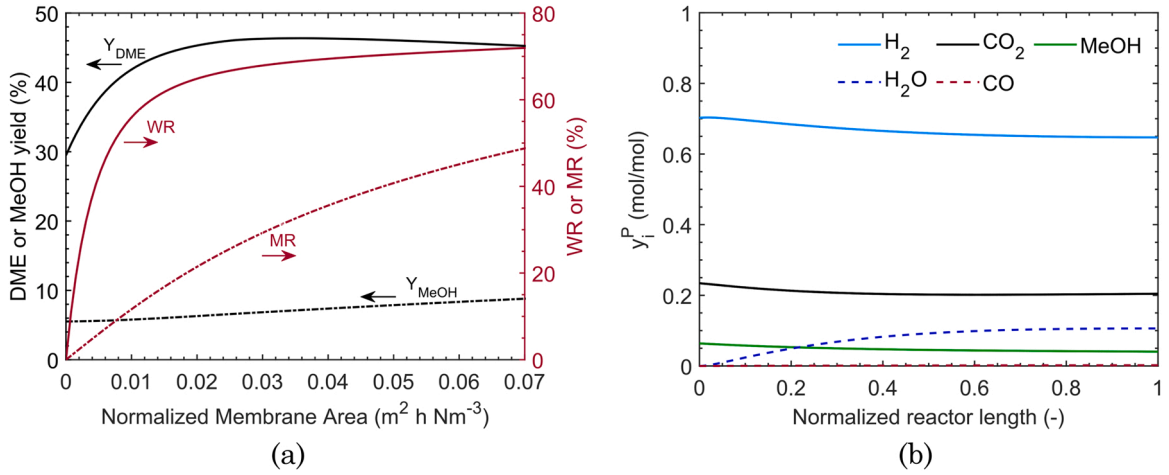

Fig. 3. PBMR performance in terms of Y_{DME} and Y_{MeOH} (on the left) and water removal (WR) and methanol removal (MR) (on the right) as a function of the normalized membrane area (a); composition of the sweep gas/permeate stream as a function of the normalized reactor length (z/L) when 6.37 mol% of methanol is incorporated in the sweep gas (b).

area of $4.11 \cdot 10^{-2}$ $m^2 \cdot h/Nm^3$ maximizes Y_{DME}. The gas composition in the permeation zone (Fig. 3b) obtained in these conditions shows that only water is effectively removed from the reaction environment. Indeed, the concentration of the component in the sweep gas (i.e., H_2, CO_2 and methanol) slightly decreases only due to the dilution effect caused by the permeation of water.

The optimal temperature of the boiling water (T_w) in this case was 178 °C (i.e., lower than that for the PBR), with a corresponding pressure of 9.6 bar. As a matter of fact, the PBMR achieves higher conversion, leading also to greater heat production. Details on the reaction unit and operating conditions of the MR-assisted DME production process are summarized in Table 6. Pressure drops are negligible (ca. 0.025 bar), similarly to the PBR.

3.2.2. *MR-assisted process description*

Fig. 4 shows the process flow diagram of the one-step CO_2 conversion to DME process via packed bed membrane reactors. CO_2 enters the plant at ambient conditions as stream 77 and it is compressed to 35 bar (i.e.,

Table 6
Characteristics of the PBMR-based reaction section in terms of size of reactors, number of reactors, catalyst bed and membrane properties and operating conditions.

Geometrical properties of the PBMR section				
Parameter	**Value**			
Number of reaction units	1			
Reactor length (L)	17.2 m			
Reactor ID (D_{ri})	3.45 m			
Reactor OD (D_{ro})	3.61 m			
Reactor shell ID (D_{si})	3.75 m			
Reactor shell OD (D_{so})	3.80 m			
Membrane ID (D_{mi})	0.007 m			
Membrane OD (D_{mo})	0.01 m			
Membrane length (L_m)	17.2 m			
Number of membranes (N_m)	783			
Reaction conditions and properties of the PBMR section				
Parameter	**Value**	**Parameter**	**Value**	
Total catalyst mass (m_{cat})	63.1 ton	CuZA/HZSM-5 mass ratio	9 kg/kg	
Catalyst particle size (d_p)	3 mm	Bed porosity (ε)	0.4 $m^3_{void}/m^3_{reactor}$	
Space velocity ($GHSV$)	64.3 h^{-1}	Catalyst dilution	1.33 kg_{SiC}/kg_{cat}	
H_2:CO_2 feed molar ratio R.[a]	3 mol/mol	Inlet flow R.[a](Φ_{in})	10294 Nm^3/h	
Inlet pressure R.[a] (P^R_{in})	40 bar	Inlet temperature R.[a](T^R_{in})	200 °C	
Inlet pressure P.[a] (P^P_{in})	35 bar	Inlet temperature P.[a](T^P_{in})	200 °C	
H_2:CO_2 feed molar ratio P.[a]	3 mol/mol	Sweep gas ratio (SW)	1 mol/mol	
BW temperature (T_w)	178 °C	Norm. memb. Area (NA_m)	0.0411	m^2·h/Nm^3
BW mass flow ($\dot{m}_w$)	1.78 ton/h	Methanol in P.[a] ($y^P_{MeOH,in}$)	0.0637 mol/mol	

[a] R. and P. stands for reaction and permeation zone, respectively.

pressure of the sweep gas of the PBMR units) via the same MCU previously described (i.e., four compressors with intermediate cooling to 35 °C). H_2 is fed to the system at 35 bar and 25 °C as stream 90 and it is split in two streams: 1) stream 91 for the reaction zone feed (51% of stream 90) and 2) stream 92 for the sweep gas make-up (49% of stream 90). With similar proportion, also the CO_2 stream at 3.5 MPa (stream 85) is split in: 1) stream 86, for the reaction zone and 2) stream 87, for the sweep gas. The H_2 and CO_2 streams directed to the reaction zone are both compressed to 40 bar via C6 and C5, respectively, and then mixed with the recycle (stream 20). The resulting stream 43 is first pre-heated to 180 °C via E1, using the heat of the effluent gas from the reaction section, and then to 200 °C (i.e., reactor inlet temperature) via E7 using HP steam. The H_2 and CO_2 streams directed to the sweep gas mixed with two recycle streams: 99% of stream 27 and the methanol separated at the top of T3 (stream 35). The resulting stream 40 is first pre-heated to 193 °C, via E4, using the heat of the permeated stream from the PBMR, and then to 200 °C via E6 using HP steam. Stream 45 and 42 are respectively fed to the reaction and permeation zone of the PBMR, which works at an average temperature of 220 °C and a pressure of 40 bar and 35 bar, respectively. The outlet stream from the reaction zone (stream 0) is re-compressed to 40 bar and cooled down to − 26 °C to recover DME in the liquid phase. This is done via three heat exchangers: E1, used to pre-heat the inlet stream to the PBMR reaction zone, and E2-E3 using cold utilities (i.e., cooling water and propylene). The flash drum (V1) separation is similar to that in the conventional plant, as well as the recycle of the gaseous stream, combined with the CO_2 recovered from the liquid phase.

The permeate stream from the PBMR (stream 21) is cooled down to 36 °C via three heat exchangers, first pre-heating the sweep gas stream (E4), then for heating the liquid phase produced via the second flash drum V2, prior to the distillation (E9) and finally with cooling water (E5). The resulting stream 24 is fed to the flash drum V2, which separates the permanent gas at the top (stream 25) from a liquid stream containing 55.6 wt% of water and 35.8 wt% of methanol at the bottom (stream 26). About 70% of the gaseous stream (stream 25) is recycled to the permeation zone (stream 27), together with the methanol stream recovered from the distillation section (stream 35), as previously mentioned. The remaining 30% (stream 28) is recycled to the reaction zone, after being compressed to 40 bar (C5).

The liquid stream from V1 (stream 6) is first used as internal utility stream in the CO_2 MCU and then fed at 70 °C to the first distillation tower T1. The distillation tower T1 operates at 40 bar and in a temperature range of 80.1 °C-220.4 °C to separate DME and CO_2 over the top (stream 12) and methanol and water at the bottom (stream 13). The DME/CO_2 stream is cooled down to 40 °C and fed to the column T2, operating at 40 bat and between 9.4 °C- 111 °C, to separate CO_2 at the top (stream 15) and to produce a *fuel* grade DME (i.e., purity of 99.91 wt %) at the bottom (stream 16). The pure DME stream is then depressurized 10 bat and cooled down to 35 °C (E16), to achieve the DME liquid storage conditions. The liquid stream from V2 (stream 26), is heated up to 200 °C (E9, E26 and E10) and then mixed with the water/methanol stream from T1, previously depressurized to 30 bar (stream 31). The resulting stream 33 is then heated to 220 °C (E11) and fed to the last distillation tower (T3), which operates at 35 bar and in a temperature range of 185–241 °C, to separate 99.9 wt% pure water at the bottom (stream 36) and 99.9 wt% pure methanol at the top (stream 35), which is recycled to the sweep gas stream, as already mentioned. Details on the mass balance of the plant (i.e., stream tables) are reported in S.I. As for the process flow diagram of the conventional process, the generation and usage of the utilities are also reported in the scheme in Fig. 4 with dotted lines. Furthermore, to facilitate their identification, the sweep gas and permeate stream (before the separation) are represented as dashed lines.

3.3. Heat integration and generation of the utilities

Fig. 5a and b depict the hot and cold composite curves obtained for the conventional and MR-assisted process, respectively, using the *pinch* method developed by Linnhoff [53] with a ΔT_{min} of 10 °C. The process minimum energy targets in terms of hot (Q_h) and cold (Q_c) duty were determined for both processes, starting from the stream thermal data (i.e., mass and energy balances). The Q_h for the conventional and MR-assisted process was very similar (i.e., 455 kW and 444 kW, respectively), with the latter being ca. 2.4% lower. As a matter of fact, the DME synthesis is an exothermic process and with the membrane reactor technology, an extra hot stream is produced (i.e., the permeate), from which it is possible to recover the heat for the cold streams. On the other hand, the Q_c of the MR-assisted process is much higher than that of the conventional process (i.e., 421 kW vs 99.3 kW), for the same reason. Indeed, also the permeate stream undergoes some separation (i.e., condensation and distillation of the liquid product), which mainly requires cooling duty. The maximum heat recovery which corresponds to the minimum energy targets is 1588 kW and 1527 kW for the conventional and MR-assisted process, respectively. The heat management of the reaction unit was not included in the construction of the composite curves. However, we should consider that the conventional process has one more reaction unit than the MR-assisted process, requiring ca. 10% more cooling duty.

Following this calculation, the heat integration within the two processes was carried out through the maximization of the internal heating and cooling (i.e., using process streams instead of external utilities) and using cooling water, refrigerants and steam when necessary. As a result, the energy saving (i.e., fraction of the maximum heat recovery target)

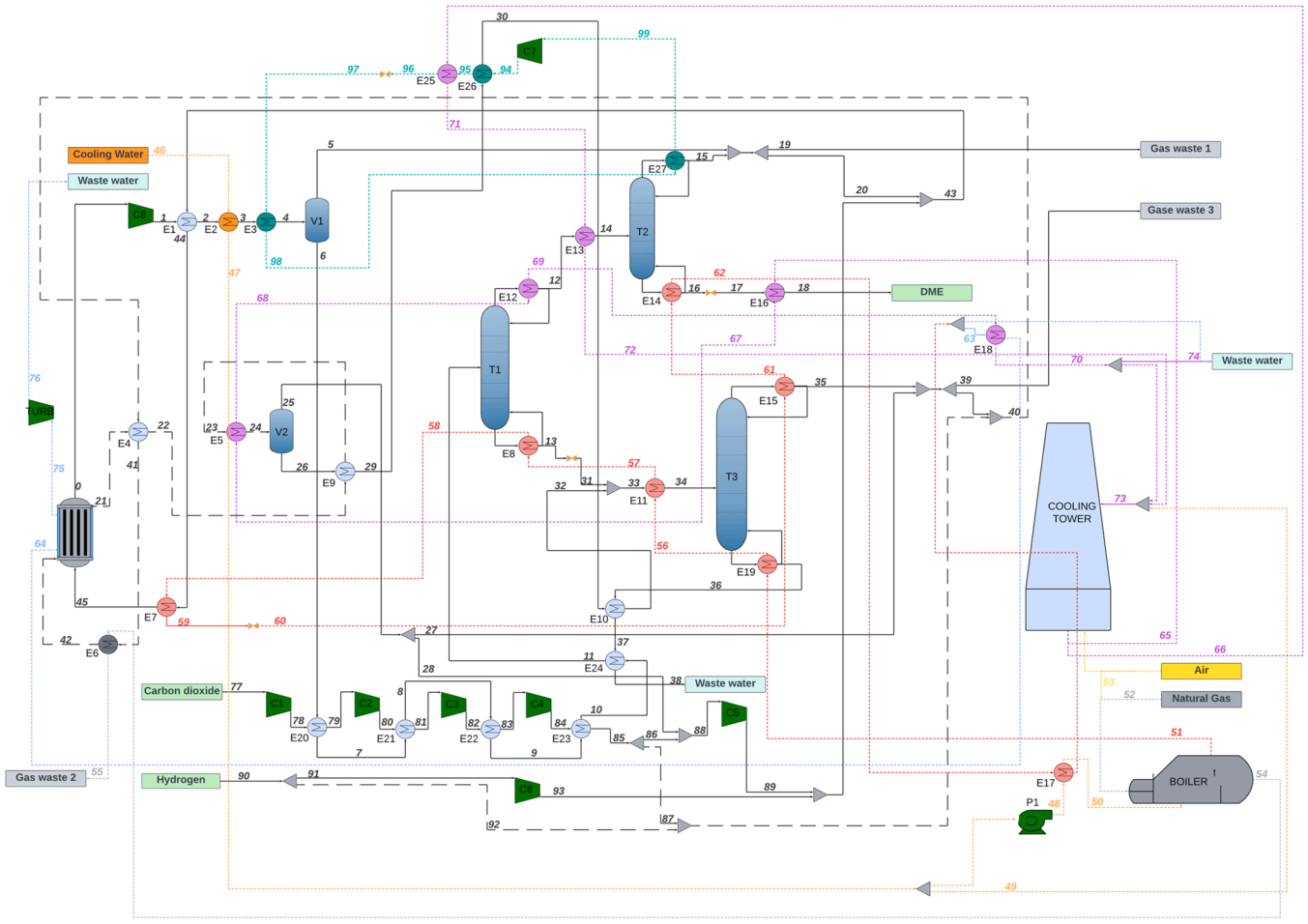

Fig. 4. Process flow diagram of the one-step CO_2 conversion to DME process via packed bed membrane reactors.

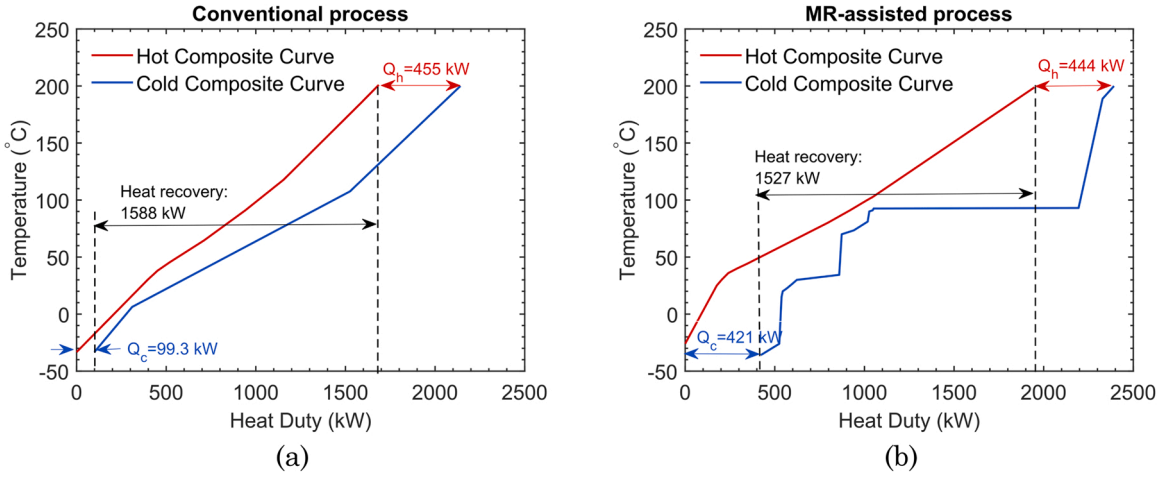

Fig. 5. Hot (red) and Cold (blue) composite curves obtained for the conventional (a) and for the membrane reactor (MR) assisted (b) one-step DME production process, obtained applying the graphical approach of the Linnhoff method [59] with a ΔT_{min} of 10 °C.

was 62.1% and 75.7% for the conventional and MR-assisted process, respectively. A general overview of the HEN of the two processes is given in Table 7. The minimum number of heat exchangers (U_{min}) was determined according to Eq. 18, where N_s is the total number of hot and cold streams, L is the number of independent loops and S is the number of independent subsystems. In our case, $L = 0$ and $S = 1$, which give the same formula proposed by Linnhoff. The amount of heat exchangers used is higher than U_{min}, due to the internal heat exchange, which allows for a reduction of the utilities and of the OPEX.

$$U_{min} = N_s + L - S \tag{18}$$

The remaining heat exchangers are based on external utilities. As described above, the flash drum V1 operates at − 33.4 °C and − 26 °C in the conventional and MR-assisted process, respectively, while the

Table 7
Heat exchangers network specifications of the conventional and MR-assisted processes.

	Conventional process	MR-assisted process
Amount of heat exchangers	21	27
Minimum number of heat exchangers	15	19
Heat exchangers with internal exchange	2	9
Heat exchangers in refrigeration cycle	2	2
Heat exchangers with cooling water	12	7
Heat exchangers with HP steam	5	9

condenser of the tower T2 operates at 5 °C in both cases. Thus, propylene is selected as cooling medium. Propylene can cool down streams till − 48 °C with a less energy intensive refrigeration cycle, when compared to ethylene. As a matter of fact, propylene requires a lower pressure to achieve its dew point at 35 °C. An overview of the refrigeration cycle is given in Table 8.

The remaining cooling duty is supplied via cooling water. Instead of using continuously fresh water, a cooling tower is implemented in both systems to further reduce the OPEX. The cooling tower cools down the water by evaporating a small portion of it, mixing warm water with air. Therefore, the outlet temperature of the water is limited by the air temperature, which in the Netherlands is 11.7 °C as yearly average, or 20 °C in the summer. For a conservative design, the air inlet temperature is set at 20 °C, which limits the water outlet temperature to 25 °C. For the heat exchangers that require a slightly lower water temperature (i.e., 15 °C), extra fresh water is fed to the system at 15 °C. This is to avoid the use of more refrigerant, which would otherwise result in a higher OPEX and CO_2 footprint. Instead, the use of more fresh water than the required make-up to the cooling tower results in some purge of warm water before being recycled to the tower. A schematic representation of the cooling water (CW) usage and recycle is given qualitatively in Fig. 6. Fresh CW enters the system at 15 °C with a flow of 9.91 ton/h and 5.40 ton/h for the conventional and MR-assisted process, respectively, to be then mixed with the corresponding 157 ton/h (43.6 °C) and 87.6 ton/h (52 °C) warm water stream from the heat exchangers network (HEN).

In both process configurations, a small portion of the warm water which is not recycled to the cooling tower is fed to a pump and a furnace, which burns natural gas and produces HP steam (i.e., steam at 40 bar and 250 °C). The HP steam production and usage is represented in detail in S.I. As the HP steam is used in the HEN, its quality decreases down to high temperature boiling water, which is used in the reaction unit for the heat management. The medium pressure (MP) steam obtained in this way is fed to a steam turbine to produce electricity. The exhaust gases produced at the furnace are used for the condenser of the tower T2 (E8) and for the pre-heating of the sweep gas (E6) in the conventional and MR-assisted process configurations, respectively. Further details on the natural gas input and electricity produced from the steam turbine are reported in Table 9.

4. Technical analysis

The two technologies proposed in this study are first compared at the

Table 8
Details of the propylene usage via the refrigeration cycle for the conventional and MR-assisted process.

	Conventional process		MR-assisted process	
	Value	Unit ID	Value	Unit ID
Propylene flow	13,045 kg/h	-	5470 kg/h	-
T_{in}/ T_{out} propylene (V1)	-48/− 46 °C	E5	-48/− 42 °C	E3
T_{in}/ T_{out} propylene (T2)	-46/− 3 °C	E21	-42/4 °C	E27
Energy for compression	788 kW	C5	327 kW	C7

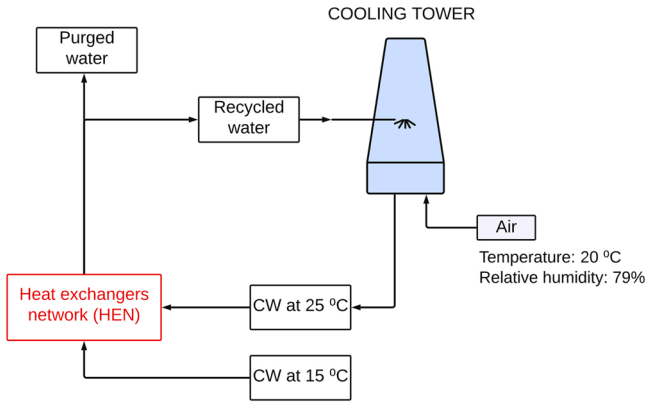

Fig. 6. Schematic representation of the cooling water usage and recycle via the cooling tower for both processes.

Table 9
Input and output of the HP steam generation and cycle for the conventional (a) and MR-assisted (b) one-step DME production process.

	Conventional process	MR-assisted process
Natural gas required (m^3/h)	281	249
Steam turbine output (kW)	260.8	197.4

reactor scale (Table 10). The membrane reactor, removing ca. 72% of the water produced in the reaction zone, allows for an increase of 41% and 63% in the $X_{CO_2 per\ pass}$ and $Y_{DMEper\ pass}$, respectively. Most importantly, the PBR and PBMR work at the same GHSV, which means that the PBMR requires ca. 40% lower mass of catalyst and flow of reactants to achieve the same DME productivity, given the higher performance of the PBMR. As a result, the membrane reactor technology allows for a reduction in the number of reaction units required to achieve a specific productivity (i.e., with the PBMR we can remove one parallel reactor). Another important aspect is that the PBMR requires 64% less H_2 per unit mass of DME produced, $\eta_{H_{2to\ DME}}$, (i.e., 0.47 and 0.78 for the PBMR and PBR, respectively). This means that the PBMR converts H_2 more efficiently, reducing the impact of one of the main cost driver, as well as bottleneck, of the hydrogenation processes. The PBMR is not only more efficient in terms of conversion/yield, but also in terms of energy efficiency and CO_2 footprint. The amount of boiling water required for the heat management is 17.3% lower than that for the PBR, which means that less energy and natural gas are required for the production of the reactor utility. Finally, the PBMR shows a *CGE* of 88% versus the 76% of the PBR, which confirms that also the energy conversion of the PBMR is more efficient.

Table 10
Key performance indicator (KPI) at the reactor level: comparison of the PBR and PBMR unit for the DME synthesis via CO_2 one-step hydrogenation.

KPI	PBR	PBMR
Number of reaction units	2	1
Catalyst mass (m_{cat})	126 ton	77.0 ton
Membrane area (A_m)	0	423 m^2
CO_2 conversion ($X_{CO_2 per\ pass}$)	38.7%	54.6%
DME yield ($Y_{DMEper\ pass}$)	32.2%	52.6%
DME selectivity (S_{DME})	83.2%	96.4%
H_2 feed ($\dot{m}^{in}_{H_2}$)	9.16 kton/y	5.59 kton/y
CO_2 feed ($\dot{m}^{in}_{CO_2}$)	66.3 kton/y	40.6 kton/y
DME productivity ($\dot{m}^{out}_{DME}$)	11.8 kton/y	12.0 kton/y
H_2 from recycle	62.4%	47.8%
CO_2 from recycle	62.3%	48.7%
$\eta_{H_{2to\ DME}}$	0.78 ton/ton	0.47 ton/ton
Boiling water mass flow ($\dot{m}_w$)	17.4 kton/y	14.4 kton/y
CGE	76.0	87.7

Table 11 compares the two process configurations (i.e., considering reactor as well as feeding and product separation section) based on their technical performance indicators evaluated from the mass and energy balances. The MR-assisted process allows for a reduction in the H_2 requirement by 15.2%, which is significantly lower that the savings anticipated based on reactor performance alone. This is due to the H_2 make-up required for the sweep gas stream. In terms of product, the two plants were designed to achieve the same productivity (i.e., 10 kton/y of *fuel* grade DME). However, the conventional process also produces 2.6 kton/y of industrial grade methanol as sellable product. On the contrary, the methanol produced in the PBMR is 100% recycled as sweep gas after its purification, to improve the DME selectivity per pass, as reported in Section 3.2.1. Thus, the resulting *CGE* of the two plants remains very similar, with only ca. 1.77% improvement of the MR–assisted over the conventional process (i.e., 89.8% vs 91.3%). Nevertheless, the energy consumption of the MR-assisted process is strikingly (i.e., 49%) lower than the conventional counterpart, mostly due to a 52% reduction of the energy requirements in the compression of the refrigeration cycle. Similarly, given the difference in size of the recycle streams (Table 10), the compression of the reactor unit effluents requires only 2.06 kW for the MR-assisted process versus the 5.01 kW of the conventional process. The pump (P1) required for the HP steam production shows a similar consumption for the two processes, while the electricity produced via the steam turbine (TURB) is ca. 24.3% lower for the MR-assisted technology, given the lower boiling water requirement for the reaction unit. The MR-assisted plant has also a lower requirement of HP steam, which corresponds to a natural gas usage ca. 11.3% lower than in the conventional plant. Overall, the MR-assisted process achieves a total energy efficiency of 72.9% versus the 69.9% of the conventional process.

When comparing the two plants in terms of the usage of the utilities per unit of DME produced (Table 12), the MR-assisted process always require a lower amount of any utility (i.e., propylene, cooling water and steam), with an overall $Z_{utilities}$ of 45.9% lower, which is mostly attributed to the lower requirement of cold utilities.

Table 11
Technical performance comparison of the conventional and MR-assisted one-step DME production process.

	Unit	Conventional process	MR-assisted process
Feedstock			
H_2	kg/h	425.8	360.9
CO_2	kg/h	3100	2629
Thermal input (W_{feed})	MW	14.19	12.03
Chemical products			
DME	kg/h	1368	1369
Purity	wt%	99.99	99.99
Methanol	kg/h	17.5	0
Purity	wt%	99.85	0
Thermal output (W_{chem})	MW	12.74	10.99
Cold Gas Efficiency (*CGE*)	**%**	**89.76**	**91.35**
Electricity			
Compressors			
MCU (CO_2)	MW	$2.563 \cdot 10^{-1}$	$2.20 \cdot 10^{-1}$
C5	MW	$7.883 \cdot 10^{-1}$	$2.27 \cdot 10^{-1}$
C6	MW	$2.416 \cdot 10^{-1}$	$1.047 \cdot 10^{-1}$
C7	MW	$5.010 \cdot 10^{-3}$	$3.724 \cdot 10^{-1}$
C8	MW	0	$2.06 \cdot 10^{-3}$
Pumps			
P1	MW	$4.18 \cdot 10^{-3}$	$4.055 \cdot 10^{-3}$
Turbines			
TURB	MW	$-2.608 \cdot 10^{-1}$	$-1.974 \cdot 10^{-1}$
Total electricity	MW	$8.17 \cdot 10^{-1}$	$4.164 \cdot 10^{-1}$
Natural gas for HP steam			
Natural gas	kg/h	193.6	171.7
Natural gas energy (W_{NG})	MW	2.634	2.336
Total energy efficiency (η)	**%**	**69.90**	**72.87**

Table 12
Efficiency of the utilities compared to the amount of DME produced for the conventional and MR-assisted process.

KPI	Conventional process	MR-assisted process
$Z_{propyl.}$	10.4	4.48
Z_{CW}	311.6	167.4
Z_{steam}	5.32	5.17
$Z_{utilities}$	**327.3**	**177.1**

The analysis of the carbon footprint is also relevant to underline the advantage of using membrane reactor technologies. Fig. 7**a** shows that the direct CO_2 emissions of the two plants is very similar (i.e., 0.04 ton_{CO_2}/ton_{DME}), in both cases attributed to the residual (ca. 1%) of the unconverted reactant streams which is not recycled. However, the direct emissions only contribute ca. 5–7% to the total CO_2 emissions. The main contributors are the electricity and steam generation (i.e., indirect emissions), which for the MR-assisted plant are 48.1% and 25.3% lower than for the conventional plant, respectively. The lower carbon footprint of the MR-assisted plant is in line with the energy balance and with the utilities requirement (Table 11).

Overall, the conventional and the MR-assisted processes emit 0.71 and 0.53 ton_{CO_2}/ton_{DME} respectively. However, when the CO_2 emissions are compared to the CO_2 fed to the plant, these numbers becomes negligible, being our technologies based on CO_2 utilization. As a result, since the conventional plant converts the feedstock with a lower efficiency at the reactor scale, thus requiring more CO_2 per unit of DME produced, the CO_2 avoided is slightly higher for the conventional plant than for the MR-assisted one (1.56 vs 1.39 ton_{CO_2}/ton_{DME}). Therefore, considering the size of the plants, the conventional and MR-assisted process avoid ca. 170 kton/y and 152 kton/y of CO_2, respectively.

Furthermore, when the one-step DME production via CO_2 hydrogenation is compared to the benchmark process (Fig. 7**b**), where DME synthesis is based on fossil fuels (i.e., syngas produced via steam reforming of natural gas), the CO_2 footprint of our technologies is between 73% and 80% lower. This means that the DME production technology proposed in this study is much more sustainable. Indeed, the CO_2 emissions for the industrial DME production range between 89 and 98 gCO_2/MJ_{DME} [13–15]. This number accounts for the NG-to-DME production pathway, independently on the direct or indirect route. When translated in terms of ton_{CO_2}/ton_{DME}, it results in an average value of 2.63. Thus, the technology we propose here is, from one hand, a valuable CO_2 utilization route and, from the other hand, a more eco-friendly pathway for the production of DME.

5. Economic analysis

The results of the economic analysis are summarised in Table 13. The purchase equipment cost (PEC) is the same for both process configurations (i.e., 1.809 M€ vs 1.802 M€). As a matter of fact, the MR-assisted process has an extra flash drum (V2) for the permeate stream and a larger number of heat exchangers of the HEN, which result in a PEC contribution increase from 3.82% to 6.53% and from 20.57% to 26.53% for the flash columns and heat exchangers, respectively. On the other hand, the MR-assisted process displays a 45.9% lower cost for the reactor section with respect to the conventional process, due to the removal of one reaction unit. The distributed PEC is graphically represented in Fig. 8**a**, where we can observe that the main contribution to the PEC is given by the compressors (i.e., 36.8% and 32.1%), followed by the heat exchangers (i.e., 20.6% and 26.5%), distillation towers (i.e., 15.1% and 15.4%) and finally the turbine (18% and 14.7%).

Considering the operating costs, the MR-assisted process has a total variable cost of 15.15 M€/y versus the 19.59 M€/y of the conventional plant, in line with the higher efficiency in converting the feedstock and

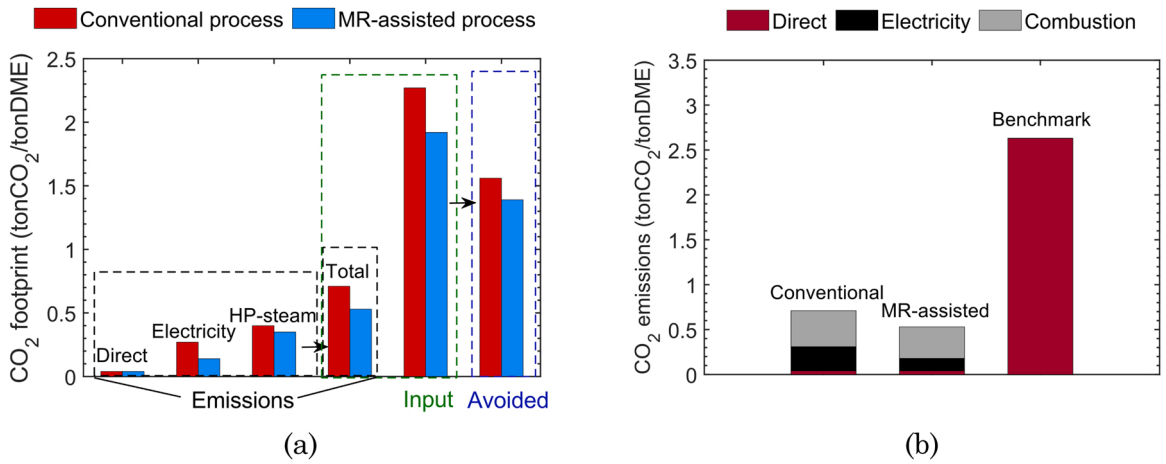

Fig. 7. CO_2 emissions and usage of the conventional and MR-assisted one-step DME production process (b) CO_2 emissions of the conventional and MR-assisted process compared to the emissions of the benchmark DME production from natural gas.

Table 13
Overview of the economic analysis for the for the conventional and MR-assisted and one-step DME production process.

Cost component	Unit	Conventional process	MR-assisted process
Initial capital investment			
PEC	**M€**	**1.809**	**1.802**
Compressors	%	36.77	32.14
Distillation towers	%	15.06	15.43
Flash columns	%	3.818	6.528
Heat exchangers	%	20.57	26.63
Reactor unit	%	1.740	0.940
Turbine	%	17.99	14.69
Furnace and boiler	%	2.834	2.877
Cooling tower	%	1.214	0.753
CAPEX	**M€**	**13.73**	**13.68**
Operating costs			
Total variable cost	**M€/y**	**19.59**	**15.15**
Catalyst	%	29.16	22.84
Membrane	%	0	1.075
Feedstock (H_2)	%	57.81	62.91
Feedstock (CO_2)	%	4.717	5.134
Utilities	%	8.315	8.040
Fixed OPEX	**M€/y**	**3.345**	**3.585**
OPEX	**M€/y**	**22.94**	**18.74**
ACAPEX	**M€/y**	**1.379**	**1.338**
TAC	**M€/y**	**24.32**	**20.08**
MDSP	**€/ton$_{DME}$**	**1960**	**1739**

the lesser utility requirement of the MR-assisted process. As shown in Fig. 8**b**, the largest contribution to the OPEX is given by the H_2 make-up, which amounts to 57.8% and 62.91% for the conventional and MR-assisted process, respectively. The second contributor to the OPEX is the catalyst cost, with a 29.2% and 22.8% of the total variable cost for the conventional and MR-assisted process. On the other hand, the cost of the utilities (mostly determined by the cost of natural gas and electricity) has a lower impact. Nevertheless, this cost is strongly affected by the geopolitical situation, which introduces some uncertainties on this number (see Section 6.6). In the base case, no carbon tax is considered, while a dedicated analysis on this subject is reported in Section 6. Therefore, the only cost related to the waste material (i.e., water in our case) is included in the utilities and consists of ca. 4% of the total utilities cost.

When comparing the OPEX with the annualized CAPEX (ACAPEX), it is clear that the impact of the capital investment on the annual costs is negligible. As a result, the TAC follows the same trend as the OPEX, with a value of 24.32 and 20.08 M€/y for the conventional and MR-assisted process, respectively. As a consequence, the minimum DME selling price (MDSP) amounts to 1960 and 1739 €/ton, respectively (i.e., ca. 11.2% reduction in MDSP in the case of the MR-assisted process). These MDSP values align with the range identified by Michailos et al. [19] (i.e., 1828–2322 €/ton). The average MDSP they found is 2193 €/ton for a two-steps DME synthesis process using conventional packed bed reactors and, likewise in this study, using captured CO_2 and H_2 from PEM as feed. By combining the two steps in a single reaction unit and with the use of the membrane reactor technology, we were able to decrease the

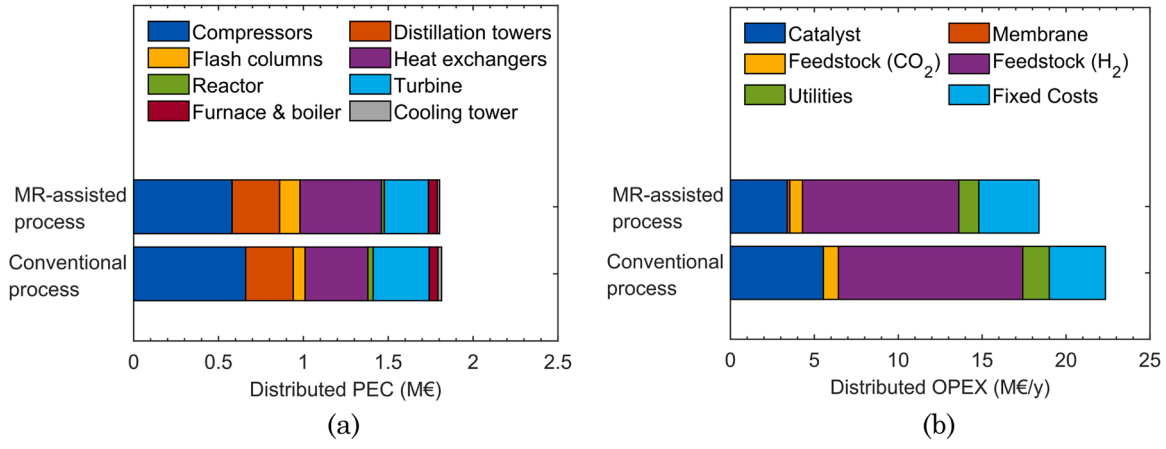

Fig. 8. Distributed PEC (a) and distributed OPEX (b) for the MR-assisted and conventional one-step DME production process.

MDSP by 1.26 times, which is a great achievement.

Nevertheless, DME is currently sold for a price of 520 €/ton, which is more than 3 times lower than our MDSP. However, the market price refers to a chemical grade DME, commonly sold as aerosol propellant or as a solvent, thus with a different market value than the fuel grade DME, despites its similar purity specification. The fuel grade DME is not on the market yet, but it is expected to be soon [69]. Thus, it is difficult to predict its value, although it would be reasonably higher than the current DME market price, to be in line with the price of diesel/LPG. Another important aspect to consider is that the DME produced via CO_2 hydrogenation would have a higher value in the perspective of a decarbonization of the fuel and chemical industry, since it derives from an alternative feedstock/waste (i.e., the captured CO_2), rather than from fossil fuels. Despites this, in the current market conditions, the production of DME from CO_2 and renewable H_2 with our technology would not be profitable. Thus, it is crucial to analyze the system in more depth, to understand the bottlenecks and to identify the conditions in which this process would become an attractive solution at industrial level.

6. Forecasting and sensitivity analysis

The economic analysis (Section 5) showed that the one-step DME production via CO_2 hydrogenation route is not yet competitive with the benchmark route (i.e., DME from steam methane reforming or SMR), given the current market conditions. However, the market conditions are expected to change due to the environmental concerns and the needs of decarbonizing the chemical industry. Therefore, in this section, we provide a detailed analysis of the possible conditions which could render our technology industrially appealing in the future.

As we learned already in Section 5, the one-step DME production via CO_2 hydrogenation is an OPEX intensive process. As a matter of fact, the ACAPEX is ca. the 5.67% and 6.66% of the TAC for the conventional and MR-assisted process, respectively. This means that the MDSP is mainly affected by the OPEX. Fig. 9 shows that the H_2 feedstock price is largest contributor to the MDSP, followed by the cost of the catalyst, which strongly depends on its lifetime. Furthermore, the cost of the natural gas as well as of the CO_2 feedstock, both show a minor and similar impact. Finally, both the membrane lifetime and the cost of the electricity do not affect the MDSP significantly. Based on this preliminary analysis, in this section we propose some sensitivity analyses on the main cost drivers, as well as further process optimization strategies to reduce the operating costs.

Finally, we suggest different realistic scenarios which could decrease the MDSP in the next few years at the point in which the DME production cost via CO_2 hydrogenation in membrane reactors balances with the forecasted DME market value.

6.1. Forecasting of H_2 price according to different production methods

The H_2 price is extremely influenced by the production method. An overview of the available technologies, together with their current cost and its prediction in 2050 is given in Table 14. The H_2 production methods can be summarized as follows: 1) H_2 from fossil fuels, which include the widely used steam methane reforming (SMR), but also higher hydrocarbon cracking, reforming and gasification; 2) H_2 from electrolysis of water, either from renewable energy and using electricity from the grid (i.e., mostly fossil fuel based). In 2010, about 96% of the H_2 used in industry was produced from fossil fuels (i.e., natural gas, coal and oil) [70]. Currently, this value is still close to 90%, being the SMR technology the cheapest on the market. The remaining 10% is mostly produced via water electrolysis, which still leads to considerable indirect CO_2 emissions, given the electricity requirement. Furthermore, these technologies are 3–10 times more expensive than the SMR, especially because these methods are still under development/optimization and they are mainly affected by the price and source of the electricity.

In our base case scenario, we assumed that H_2 is supplied by an integrated pipeline network (i.e., H_2 price of 2.95 €/kg, as reported by Fortes et al. [39]), with H_2 being mostly produced via steam methane reforming and coal and biomass gasification coupled with CCS. Despites the CCS technology, these production routes are energy intensive, thus, not environment-friendly. The goal of this research is to promote a sustainable production method of DME, as well as a route for the CO_2 utilization. As a result, we should also consider the impact of any indirect CO_2 emission source, such as the emission related to the H_2 production. The only production method which can potentially be 100% renewable is the electrolysis. However, when the electricity from the grid is used, H_2 cannot be considered as renewable. As a matter of fact, nowadays, still 80% of the electricity in the Netherlands is produced using fossil fuels with a CO_2 footprint of 330 gCO_2/kWh [71].

Table 14
Current Price of H_2 and its prediction in 2050 according to different production methods.

Production method	Type[a]	Current cost	Cost in 2050	Ref.
Fossil fuels (SMR)	H_2	1.3 €/kg	-	[73]
Electrolysis[b]	H_2	2.50–6.7 €/kg	-	[74]
Electrolysis (AE)	REN- H_2	5.6 €/kg	2.12 €/kg	[72]
Electrolysis (PEM)	REN- H_2	7.1 €/kg	1.81 €/kg	[72]
Electrolysis (SOE)	REN- H_2	6.0 €/kg	1.03 €/kg	[72]
Electrolysis (PEC)	REN- H_2	10.8 €/kg	1.91 €/kg	[72]

[a] H_2 from 100% renewable resources is classified as REN-H_2 [72].
[b] In some studies grid-electricity is used, sometimes in combination with renewable energy, so the H_2 production is not 100% renewable.

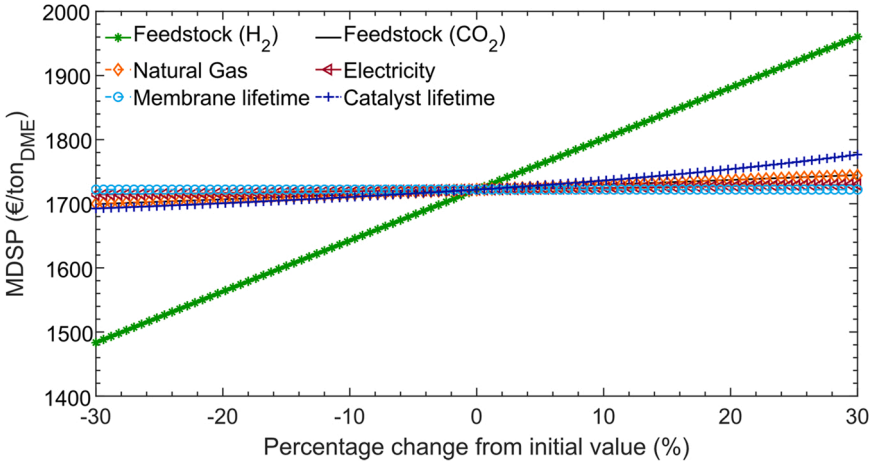

Fig. 9. Effect of the higher impact cost drivers of the OPEX on the MDSP of the MR-assisted one-step DME production process.

To remove any source of CO_2 emission, H_2 must be produced via electrolysis based on 100% renewable resources, which makes the H_2 production much more expensive (Table 14). At the moment, the alkaline electrolysis (AE) is the most mature technology and, as a consequence, the cheapest sustainable route. Polymer electrolyte membrane (PEM) electrolysis is approaching the cost of the AE and even the MW-scale systems are currently market ready [72]. On the other hand, the solid oxide electrolyser (SOE) technology is not yet ready for the industrial scales. Detz et al. [72] predicted the H_2 price from different sustainable technologies in the time span from 2015 to 2050, considering that phenomena such as learning-by-doing, learning-by-searching, economies-of-scale, and automation can reduce the renewable H_2 manufacturing costs. According to their prediction, both PEM and SOE are the techniques that in the future (i.e., by 2050) will be able to produce H_2 at comparable prices (i.e., 1.3 €/kg) to the fossil fuel based technologies.

Therefore, we implemented in our economic analysis the function derived by Detz et al. describing the decrease in the H_2 price within the years for both the PEM and SOE technologies. The effect of changing the H_2 price on the MDSP for both the conventional and MR-assisted process is depicted in Fig. 10, where it is clear that the choice of the electrolysis method between PEM and SOE has a large impact on the MDSP and that, despites the readiness of the technology, the SOE is much more promising in terms of economics. Furthermore, we observe that the MDSP of the MR-assisted technology is always much lower than the one related to the conventional process. As a result, in the next analyses, we will consider only the MR-assisted technology with the H_2 obtained via SOE as a new base case scenario.

6.2. Effect of the carbon tax

As learned in Section 6.1, with the prediction of the H_2 price by SOE, the MDSP of the MR-assisted technology can be reduced to 1376 €/ton in 2050. This price cannot be directly compared to the DME market price, which corresponds to the benchmark technology. As a matter of fact, the DME production cost from SMR is expected to increase in the next years, due to the extra costs related to the emissions and the corresponding carbon tax. Indeed. the carbon tax in the Netherlands and in Europe (on average) is expected to increase linearly over the years (Fig. 11**a**) [45]. With this data, the DME market price can be estimated over the years, considering an average emission of 93 gCO_2/MJ_{DME} [13–15] and assuming that after 2030, the carbon tax will continue to increase linearly (i.e., linear extrapolation). However, in this analysis we assume that no carbon tax is included in the current DME market price (year 2020) and that the price of other feedstock, like natural gas, are not influenced by the carbon tax significantly. On the other hand, the effect of the carbon tax on the MDSP related to the one-step DME production via CO_2 hydrogenation is more complex to analyse. We should consider that our system uses CO_2 as a feedstock. This implies that the carbon tax can have: 1) a negative effect, due to the CO_2 total emissions and 2) a positive effect on the reduction of the CO_2 feedstock price. The latter effect is described in Section 6.5. When considering, at the same time, the reduction in the H_2 price from SOE and the negative effect of the carbon tax on the MDSP of the MR-assisted technology, as well as the effect of the carbon tax on the DME market price, a competitiveness curve can be obtained (Fig. 11**b**) showing that the novel technology based on CO_2 utilization will be competitive with the benchmark method in 2050.

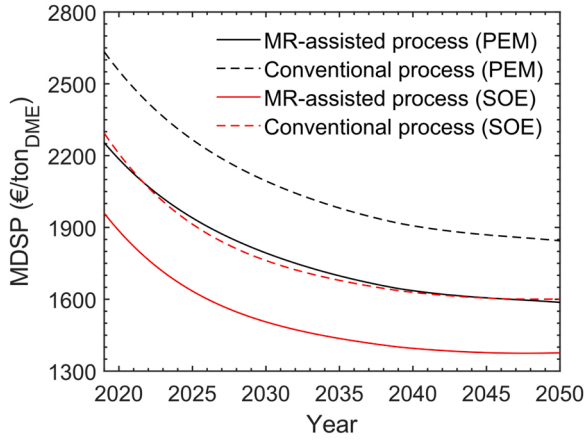

Fig. 10. MDSP for the conventional (dashed lines) and MR-assisted plant (solid lines) as a function of time (years) considering different H_2 production technologies: PEM (black lines) and SOE (red lines), implementing the H_2 price predicted by Detz et al. [72].

6.3. Effect of the catalyst lifetime (scenario 1)

The $Cu/ZnO/Al_2O_3$-HZSM-5 catalyst we selected in this study has a lifetime of ca. 2 years, as reported in literature [19,75]. Its deactivation phenomena usually arise from copper crystallization and aluminum leaching with hot water, possible poisoning from sulfur based compound (i.e., impurities in the feedstock) and coke formation, which is faster and enhanced at higher temperatures (i.e., above 300 °C [76]). However, the catalytic bed of the membrane reactor operates in an almost dry environment, given the removal of water by means of the membrane module. Furthermore, we promote a low temperature operation process (i.e., an average reactor temperature of 220 °C, with a peak at 260 °C), given the more severe thermodynamic limitations when using pure CO_2 as the sole carbon source and the higher efficiency of the PBMR. As a result, the catalyst deactivation could be reasonably delayed and its lifetime can be extended from 2 to 5 years, to be compatible with the lifetime of the membranes. Considering a catalyst lifetime of 5 years, the MDSP curve referred to the MR-assisted technology of Fig. 11b will shift downwards of ca. 192 €/ton (scenario 1), becoming even more attractive than the conventional technology and crossing the DME market price already in 2043 (i.e., 7 years earlier).

6.4. Optimization of the HP steam cycle and natural gas usage (scenario 2–4)

The third important cost contributor to the MDSP is the cost of natural gas (NG), which also directly influences the CO_2 emissions related to the combustion. The natural gas requirements can be reduced by optimizing the use of the HP steam, which is mainly required at the reboiler of columns T1 and T3. As seen also in Table 13, the CAPEX has a small impact on the TAC and on the MDSP. Therefore, we could increase the number of stages of the distillation tower T1 to reduce the reflux ratio and, as a result, the reboiler duty. An increase in the number of stages from 18 to 22 corresponds to a decrease in the reflux ratio from 5 to 4 (beyond 22 stages, the reflux ratio changes are not significant). This condition corresponds to a reduction of 15.5% and 12% in the HP steam flow and natural gas requirement, respectively, as well as to a CAPEX increase of 0.06%, which has a negligible effect on the MDSP. On the other hand, we did not find any beneficial effect in increasing the height of the column T3.

Based on the optimized usage of the HP steam, multiple scenarios can be built, on top of scenario 1 (i.e., considering a catalyst lifetime of 5 years):

- Scenario 2: Natural gas is used for the production of the HP steam in the optimized conditions (i.e., 12% NG usage less than the base case);
- Scenario 3: The purge stream of the unconverted gases, which still contains a heating value of ca. 1175 MJ/h due to the presence of H_2 (70 mol.%) and traces of CO, methanol and DME, can be fed to the burner, in combination with a reduced flow of natural gas. This solution further reduces the NG usage of 20%;

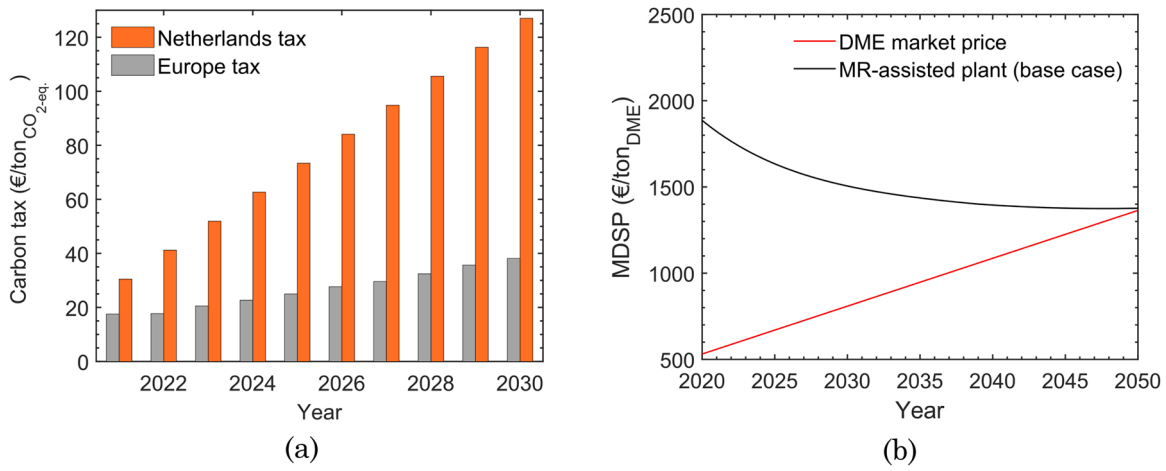

Fig. 11. The expected carbon tax for the coming years on average in Europe (grey bars) and in the Netherlands (orange bars) (a); MDSP of the MR-assisted plant (solid lines) as a function of time (years) when compared with the DME market price prediction (red line).

- Scenario 4: The natural gas required in scenario 3 is completely replaced with green H_2. As a result, the purge stream is fed to the burner together with H_2. This solution also minimizes the CO_2 emissions.

An overview of the NG requirement and the alternative fuels used for the production of the HP steam in the base case and three scenarios is given in Table 15, together with the impact on the direct CO_2 emissions. The impact of the three scenario on the competitiveness curve is depicted in Fig. 12. The MDSP curve related to scenario 2 and 3 decrease over the years with the same trend of the base case (i.e., curve of Fig. 11**b**). However, these curves are only slightly shifted downwards due to the lower NG consumption, since in general we saw that the impact of the NG cost on the total OPEX is not that significant. On the other hand, the curve representing scenario 4 decreases with a quite different slope, due to the implementation of the H_2 decreasing function, together with the reduction of the NG usage and the CO_2 emissions. For the same reason, scenario 4 has initially a higher MDSP than the other scenario, because of the higher cost of H_2 used for the combustion. Nevertheless, with the decrease in the H_2 price over the years and with the increase in the carbon tax, the MDSP decreases faster than the other cases from the year 2025, anticipating the moment from which our technology will be competitive with the benchmark of ca. 3 years (i.e., 2040 instead of 2043).

6.5. *Effect of the CO_2 feedstock price: carbon capture vs carbon tax (scenario 5–7)*

Although the CO_2 feedstock price does not play a significant role on the MDSP, similarly to the natural gas, we believe that this variable needs a dedicated section. As a matter of fact, the technology we propose here uses CO_2 as the sole carbon source for the synthesis of DME.

Table 15
Overview of NG requirement and the alternative fuels used for the production of the HP steam in the base case and the three scenarios, together with the corresponding direct CO_2 emissions.

	Base case	Scenario 2	Scenario 3	Scenario 4
Natural gas/DME (ton/ton)	0.13	0.11	0.09	0
Purge streams/DME (ton/ton)	0	0	0.05	0.05
REN-H_2/DME (ton/ton)	0	0	0	0.03
CO_2 emissions/DME (ton/ton)	0.39	0.35	0.31	0.05

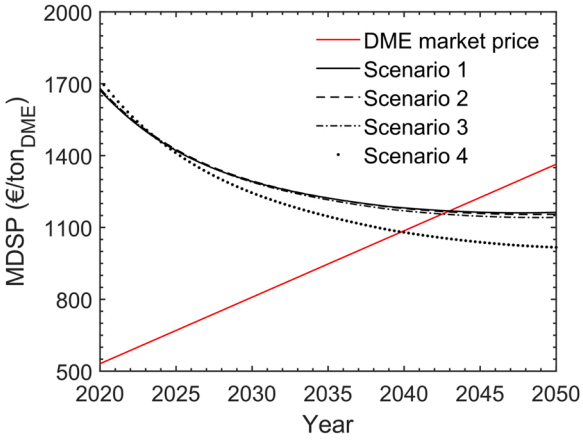

Fig. 12. MDSP of the MR-assisted plant (black lines) as a function of time (years) when compared with the DME market price prediction (red line), using REN-H_2 from SOE, a catalyst life time of 5 years in the three scenario for the HP steam production.

Therefore, we could easily imagine a future scenario in which, heavy CO_2 emitting companies would be keen to buy our CO_2 utilization technology to make profit from a waste rather than paying a tax. In our base case, we assumed a CO_2 feedstock price of 33 €/ton (i.e., CO_2 from SEWGS). Nevertheless, the CO_2 price is expected to change over the years due to the development of the CO_2 capture technologies and to the environmental concerns and the corresponding carbon tax policy. From the moment in which the carbon tax will be higher than the carbon capture price (CCP), companies will start to capture their CO_2 and either sell it or use it directly. We define this moment as t_1, which allows us to identify two different time regions: 1) Before t_1, the price of the CO_2 feedstock for our technology corresponds ca. to the CCP, since we have to buy it from industries/companies which decide to capture CO_2 and sell it with a certain profit. Indeed, industries will not capture their CO_2 for "free", since paying a carbon tax would be cheaper; 2) After t_1, the situation is more complex and we can identify three scenario:

- Scenario 5: after t_1 the CO_2 feedstock price will be zero;
- Scenario 6: after t_1 the CO_2 feedstock price will correspond to the difference between the carbon tax and the CCP. As a result, the CO_2 feedstock will be seen as a revenue instead of a cost. Indeed, companies would prefer to capture the CO_2, rather than paying a tax, and

would pay the difference for the CO_2 utilization process, which could be seen as a waste treatment technology.

- Scenario 7: it is similar to scenario 6, but with a slightly different revenue. The company which decides to capture the CO_2 instead of paying the carbon tax, would prefer to pay for the CO_2 utilization technology less than the difference between the carbon tax and the CCP. This scenario is much more realistic, since it is easy to imagine that if the CO_2 waste treatment and the carbon tax come with the same price, one would still prefer to pay a tax and avoid further capital investments in CO_2 capture technologies. In this scenario we assume that the CO_2 emitting companies would pay 14.1% less than the difference between carbon tax and CCP. This % corresponds to the average gross profit margin of primary metal industry [77].

These scenario can be built on top of scenario 4, described in the previous section, where the usage of the HP steam and of the fuels to produce it are optimized.

Within these scenario, we do not consider the case in which, after t_1, the CO_2 emitting companies would decide only to sell it with a profit margin, since this will correspond exactly to our scenario 4, with the CO_2 feedstock price of the base case. Nevertheless, it is easy for us to see the CO_2 feedstock as a revenue, since when the CCP is lower than the carbon tax, it is worth for the companies to capture the CO_2. When more and more companies will capture their CO_2, the market will be saturated and if they cannot sell it, they would still need to emit it and pay the carbon tax on top of the CCP. As a result, these companies would be willing to pay a difference between carbon tax and CCP to the CO_2 consumers.

The competitiveness curve related to the new scenario (5, 6 and 7), together with the one of scenario 4 (see Section 6.5), are depicted in Fig. 13. Scenario 5, 6 and 7 were all built on top of scenario 4, which was the best scenario found in view of the optimization of the HP steam generation and usage. Starting from 2022 the curves related to the new scenario show a discontinuity, due to a drop in the price of the of CO_2 feedstock. As a result, the year 2022 corresponds to t_1, where the carbon tax has achieved the CCP (i.e., 33 €/ton for the SEWGS). From this point on, it is clear that scenario 6 is more convenient, followed by scenario 7 and scenario 5. In case of scenario 6 and of the more realistic scenario 7, our MR-assisted process could become competitive with the benchmark already in 2032 and 2033, respectively. In case of scenario 5, instead, our process would be competitive in 2038.

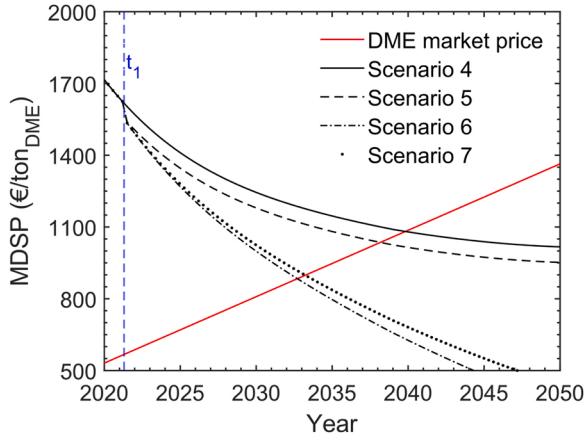

Fig. 13. MDSP of the MR-assisted plant (black lines) as a function of time (years) when compared with the DME market price prediction (red line), using REN-H_2 from SOE, a catalyst life time of 5 years, H_2 and purge streams for the HP steam production in the three scenario identified for the CO_2 feedstock price. The blue dashed vertical line represents the time t_1.

6.6. Overview and uncertainty analysis

Table 16 gives an overview of the scenario built in Sections 6.4 and 6.5, in terms of the MDSP, year and carbon tax corresponding to the intersection point between the MDSP curve and the DME benchmark market price (i.e., moment in which the one-step DME synthesis via CO_2 hydrogenation using membrane reactors will become competitive with the benchmark DME synthesis). According to this analysis, our technology could become profitable, and thus industrially applicable, between 2040 and 2032. As a matter of fact, scenario 1 considers a longer catalyst lifetime, which is realistic thanks to the advantages of the membrane reactor technology, as discussed in Section 6.3. Furthermore, scenario 2–4 depends on an optimization of the fuel used for producing HP steam. Therefore, it is reasonable to consider scenarios on top of scenario 4. Nevertheless, the results reported in Table 16 also show that the moment in which our technology will become competitive with the benchmark not only depends on the different scenarios, but also on the value of the carbon tax. Currently, the carbon tax policy has not been accepted all over the world and its value depends on national regulations. As an example, if we focus on the European countries who have already imposed a carbon tax, we can have a value ranging from 116.33 €/ton$_{CO_2}$ for Sweden, to a value of 0.07 €/ton$_{CO_2}$ for Poland [78]. If we consider the carbon tax corresponding at year 2020 as a variable and consider a linear increase with time as in Fig. 11**a**, the point of intersection of the MDSP of scenario 6 (i.e., the more realistic) shifts. As a result, the year of competitiveness and the corresponding carbon tax value correlates as depicted in Fig. 14, from which we can observe that the carbon tax has to be at least 118 €/ton$_{CO_2}$ to have a MDSP equal to the DME market price by 2050.

The results that we show in this section are based on several hypotheses. Although all the variables are based on previous studies and information retrieved from literature, there are some uncertainties which will surely affect the moment in which the technology would become competitive with the DME market value. A list of some of the unknown variables or data which have not been included or have been assumed in this research and that we believe could reduce the accuracy of our prediction is given here:

- The salary change over the years was not taken into account. The salary could increase due to the inflation and increase in the welfare, as example. As a result, it is very difficult to predict its future trend.
- Currently, only the price of the DME chemical grade is known. However, our technology produces a fuel grade DME, which is expected to have a higher market value.
- In case the H_2 production would be integrated in the DME synthesis, the heat generated in the hydrogen production step could be used to replace HP steam completely. As a matter of fact, the SOE process operates at temperature of 500–850 °C and the heat corresponding to the H2 stream could be used for the reboilers in the distillation towers. Furthermore, the maximum working pressure of the SOE and PEM can vary in a wide range (35–200 bar) [79,80]. This indicates that the cost of compression could be further reduced. However, the electricity cost, as well as the CAPEX, did not show a large impact on the MDSP.
- Our analysis does not take into account the possible subsidies related to the use of renewable feedstock/energy. This could reduce our cost significantly and make our system more competitive with the benchmark.
- The carbon tax in the Netherlands (30 €/ton$_{CO_2}$) is above the European average (24 €/ton$_{CO_2}$), which makes it harder for our technology to be competitive.
- The carbon capture price is also expected to be dependent on the technology adopted and on the composition of the waste stream from which the CO_2 needs to be purified. A more expensive technology would delay the moment from which CO_2 could become a cost zero feedstock or even a revenue (t_1). However, as for the H_2, also the CCP

Table 16
Overview of the different scenario in terms of MDSP, year and carbon tax corresponding to the intersection point between the MDSP curve and the DME benchmark market price.

Intersection point	Base case	1	2	3	4	5	6	7
MDSP (€/ton$_{DME}$)	1376	1179	1179	1159	1083	1038	885	900
Year	2050	2043	2043	2042	2040	2038	2032	2033
Carbon tax (€/ton$_{CO_2}$)	260	260	260	250	230	211	154	161

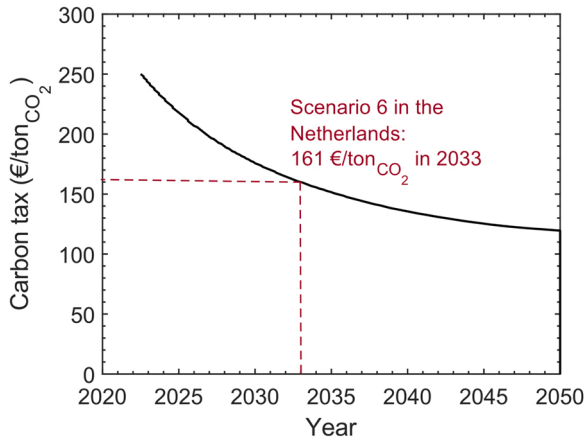

Fig. 14. Carbon tax corresponding at the year in which our technology will be competitive with the benchmark according to scenario 6, depending on the initial policy on the carbon tax (i.e., at 2020).

is expected to decrease with time, due to the development of the existing or even more efficient technologies. As an example, the use of membrane separation technologies can reduce the cost of solvent based technologies of ca. 28% [81].

- Changes in the price of natural gas over the years have not been considered in this study. However, the scenarios 4–7 are not affected by this cost, given that the natural gas has been completely replaced with renewable H_2.

7. Conclusions

This work demonstrates that CO_2 can be upgraded from a polluting agent into a valuable feedstock at industrial scale. The use of a membrane reactors (MR) in the direct CO_2 hydrogenation to dimethyl ether (DME) shifts the single pass conversion from 39% to 55%, together with a shift in the DME yield from 32% to 53%. The higher efficiency in the conversion of the packed bed membrane reactor (PBMR) allows for a remarkable decrease in both the catalyst mass and in the H_2 feedstock flow to produce 1 ton of DME of ca. 39% and 64%, respectively. Overall, the PBMR displays a cold gas efficiency (*CGE*) of 88% with respect to the 76% of the packed bed reactor (PBR). On a process perspective, the MR-assisted plant requires less energy input to produce the same amount of DME.

On the economic aspect, both processes revealed to be OPEX intensive, with the operating costs of the MR-assisted process significantly lower (ca. 23%), due to the lower requirement of H_2, which covers more than 60% of the OPEX.

The minimum DME selling price (MDSP) was found to be 1739 €/ton and 1960 €/ton for the MR-assisted and the conventional process, respectively, in the base case scenario, where no carbon tax is taken into account and the CO_2 feedstock is considered as a cost. This result proves that the combination of the two steps in a single reactor, together with the use of the membrane reactor technology, allows for a reduction in the MDSP of 1.26 times with respect to what reported in literature.

Nevertheless, the MDSP of the MR-assisted technology is still 3.3 times higher than the current DME market value. As a result, we carried out a feasibility study to predict the moment in which this technology would become competitive with the benchmark. Our analysis showed that if we consider the reduction in the H_2 price produced using the solid oxide electrolysis (SOE) technology, together with an increase in the catalyst lifetime from 2 to 5 years and an optimization of the high pressure steam and natural gas usage, our system can be competitive with the benchmark in 2040, if the carbon tax would increase linearly. In addition, if the CO_2 feedstock is considered as a revenue rather than a cost, our process could be profitable ca. 7 years earlier. The result of the competitiveness analysis strongly depends on the carbon tax policy, which varies from country to country. Overall, we conclude that, given the uncertainties related to this prediction, we can identify a region, more than an exact moment, which goes from 2025 to 2050 where the CO_2 direct hydrogenation to DME in membrane reactors will be economically competitive with the benchmark process.

CRediT authorship contribution statement

S. Poto: Conceptualization, Data curation, Formal analysis, Investigation, Writing – original draft, **T. Vink**: Investigation, Analysis. **P. Olivier**: Writing – review & editing, **F. Neira D'Angelo**: Supervision, Writing – review & editing, Methodology, **F. Gallucci**: Funding acquisition, Project administration, Resources, Supervision, Writing – review & editing, Methodology.

Declaration of Competing Interest

The authors declare that they have no known competing financial interests or personal relationships that could have appeared to influence the work reported in this paper.

Data Availability

Data will be made available on request.

Acknowledgements

This project has received funding from the European Union's Horizon 2020 research and innovation programme under grant agreement No 838014 (*C2Fuel* project).

Appendix A. Supporting information

Supplementary data associated with this article can be found in the online version at doi:10.1016/j.jcou.2023.102419.

References

[1] U.S. Global Change Research Program, Climate science special report: Fourth national climate assessment, volume I., 2018.
[2] Megan Baynes, COP26: The key agreements from Glasgow's climate summit, 2021.

[3] J.C.M. Pires, F.G. Martins, M.C.M. Alvim-Ferraz, M. Simões, Recent developments on carbon capture and storage: an overview, Chem. Eng. Res. Des. vol. 89 (9) (2011) 1446–1460.
[4] J. Ma, et al., A short review of catalysis for CO_2 conversion, Catal. Today vol. 148 (3–4) (2009) 221–231.
[5] D. Chery, V. Lair, M. Cassir, Overview on CO 2 valorization: challenge of molten carbonates, Front. Energy Res. vol. 3 (OCT) (2015) 1–10.
[6] J. Liu, K. Li, Y. Song, C. Song, X. Guo, Selective hydrogenation of CO2to hydrocarbons: effects of Fe3O4particle size on reduction, carburization, and catalytic performance, Energy Fuels vol. 35 (13) (2021) 10703–10709.
[7] K.P. Kuhl, T. Hatsukade, E.R. Cave, D.N. Abram, J. Kibsgaard, T.F. Jaramillo, Electrocatalytic conversion of carbon dioxide to methane and methanol on transition metal surfaces, J. Am. Chem. Soc. vol. 136 (40) (2014) 14107–14113.
[8] Z. Azizi, M. Rezaeimanesh, T. Tohidian, M. Reza, Chemical engineering and processing: process intensification dimethyl ether: a review of technologies and production challenges, Chem. Eng. Process. Process. Intensif. vol. 82 (2014) 150–172.
[9] M. De Falco, M. Capocelli, A. Basile, C.B. Roma, ScienceDirect Selective membrane application for the industrial one-step DME production process fed by CO 2 rich streams: modeling and simulation, Int. J. Hydrog. Energy vol. 42 (10) (2017) 6771–6786.
[10] M. Gadek, R. Kubica, E. Jedrysik, Production of Methanol and Dimethyl ether from biomass derived syngas - a comparison of the different synthesis pathways by means of flowsheet simulation, Comput. Aided Chem. Eng. vol. 32 (2013) 55–60.
[11] R. Vakili, R. Eslamloueyan, Optimal design of an industrial scale dual-type reactor for direct dimethyl ether (DME) production from syngas, Chem. Eng. Process. Process. Intensif. vol. 62 (2012) 78–88.
[12] G. Iaquaniello, G. Centi, A. Salladini, E. Palo, S. Perathoner, L. Spadaccini, Waste-to-methanol: process and economics assessment, Bioresour. Technol. vol. 243 (2017) 611–619.
[13] R. K. D. and H. H. Edwuards R. larivé J., Rickeard D., Weindorf W., GOdwin S., Hass H., Krasenbrink A., Lonza L., Nelson L. Reid A., Well-to-tank report version 4. a: Jec well-to-wheels analysis (LD-NA-26237-EN-N), 2014.
[14] D. Berkely, California Dimethyl Ether Multimedia Evaluation Tier I., 2015.
[15] U. Lee, et al., Well-to-wheels emissions of greenhouse gases and air pollutants of dimethyl ether from natural gas and renewable feedstocks in comparison with petroleum gasoline and diesel in the United States and Europe, SAE Int. J. Fuels Lubr. vol. 9 (3) (2016) 546–557.
[16] E.S. Yoon, C. Han, A review of sustainable energy - recent development and future prospects of Dimethyl Ether (DME), Comput. Aided Chem. Eng. vol. 27 (C) (2009) 169–175.
[17] P.J. Megia, A.J. Vizcaino, J.A. Calles, A. Carrero, Hydrogen production technologies: from fossil fuels toward renewable sources. A mini review, Energy Fuels vol. 35 (20) (2021) 16403–16415.
[18] E. Kusrini, W.W. Prihandini, F.A. Jatmoko, A. Usman, and Y. Muharam, Feasibility study of CO2purification using pressure swing adsorption and triethylene glycol absorption for enhanced oil recovery, AIP Conf. Proc., vol. 2255, no. September, 2020.
[19] S. Michailos, S. Mccord, V. Sick, G. Stokes, P. Styring, Dimethyl ether synthesis via captured CO 2 hydrogenation within the power to liquids concept: a techno-economic assessment, Energy Convers. Manag. vol. 184 (October 2018) (2019) 262–276.
[20] S.G. Jadhav, P.D. Vaidya, B.M. Bhanage, J.B. Joshi, Catalytic carbon dioxide hydrogenation to methanol: a review of recent studies, Chem. Eng. Res. Des. vol. 92 (11) (2014) 2557–2567.
[21] X.M. Liu, G.Q. Lu, Z.F. Yan, J. Beltramini, Recent advances in catalysts for methanol synthesis via hydrogenation of CO and CO_2, Ind. Eng. Chem. Res. vol. 42 (25) (2003) 6518–6530.
[22] C. Federsel, R. Jackstell, M. Beller, State-of-the-art catalysts for hydrogenation of carbon dioxide, Angew. Chem. - Int. Ed. vol. 49 (36) (2010) 6254–6257.
[23] R. Guil-López, et al., Methanol synthesis from CO_2: a review of the latest developments in heterogeneous catalysis, Mater. (Basel) vol. 12 (23) (2019).
[24] G. Bonura, F. Arena, G. Mezzatesta, C. Cannilla, L. Spadaro, F. Frusteri, Role of the ceria promoter and carrier on the functionality of Cu-based catalysts in the CO_2-to-methanol hydrogenation reaction, Catal. Today vol. 171 (1) (2011) 251–256.
[25] M. Mollavali, F. Yaripour, H. Atashi, S. Sahebdelfar, Intrinsic kinetics study of dimethyl ether synthesis from methanol on γ-Al2O3 catalysts, Ind. Eng. Chem. Res. vol. 47 (9) (2008) 3265–3273.
[26] E. Catizzone, A. Aloise, M. Migliori, G. Giordano, Dimethyl ether synthesis via methanol dehydration: effect of zeolite structure, Appl. Catal. A Gen. vol. 502 (2015) 215–220.
[27] S. Hosseininejad, A. Afacan, R.E. Hayes, Catalytic and kinetic study of methanol dehydration to dimethyl ether, Chem. Eng. Res. Des. vol. 90 (6) (2012) 825–833.
[28] K.W. Jun, H.S. Lee, H.S. Roh, S.E. Park, Catalytic dehydration of methanol to dimethyl ether (DME) over solid-acid catalysts, Bull. Korean Chem. Soc. vol. 23 (6) (2002) 803–806.
[29] G. Bonura, et al., Acidity control of zeolite functionality on activity and stability of hybrid catalysts during DME production via CO_2 hydrogenation, J. CO_2 Util. vol. 24 (October 2017) (2018) 398–406.
[30] P. Rodriguez-Vega, et al., Experimental implementation of a catalytic membrane reactor for the direct synthesis of DME from H2+CO/CO_2, Chem. Eng. Sci. vol. 234 (2021).
[31] A. Ateka, P. Rodriguez-Vega, T. Cordero-Lanzac, J. Bilbao, A.T. Aguayo, Model validation of a packed bed LTA membrane reactor for the direct synthesis of DME from CO/CO_2, Chem. Eng. J. vol. 408 (October 2020) (2021).
[32] M. Farsi, A. Hallaji Sani, P. Riasatian, Modeling and operability of DME production from syngas in a dual membrane reactor, Chem. Eng. Res. Des. vol. 112 (2016) 190–198.
[33] N. Diban, A.M. Urtiaga, I. Ortiz, J. Erenãa, J. Bilbao, A.T. Aguayo, Improved performance of a PBM reactor for simultaneous CO_2 capture and DME synthesis, Ind. Eng. Chem. Res. vol. 53 (50) (2014) 19479–19487.
[34] S. Poto, F. Gallucci, M.F. Neira, Direct conversion of CO 2 to dimethyl ether in a fixed bed membrane reactor: Influence of membrane properties and process conditions, Fuel vol. 302 (February) (2021), 121080.
[35] M. De Falco, M. Capocelli, A. Giannattasio, Membrane reactor for one-step DME synthesis process: Industrial plant simulation and optimization, J. CO_2 Util. vol. 22 (July) (2017) 33–43.
[36] H. Hamedi, T. Brinkmann, Valorization of CO_2 to DME using a membrane reactor: a theoretical comparative assessment from the equipment to flowsheet level, Chem. Eng. J. Adv. vol. 10 (January) (2022), 100249.
[37] K. Atsonios, K.D. Panopoulos, E. Kakaras, Investigation of technical and economic aspects for methanol production through CO_2 hydrogenation, Int. J. Hydrog. Energy vol. 41 (4) (2016) 2202–2214.
[38] J. Zhang, Z. Li, Z. Zhang, R. Liu, B. Chu, B. Yan, Techno-economic analysis of integrating a CO2Hydrogenation-to-methanol unit with a coal-to-methanol process for CO2Reduction, ACS Sustain. Chem. Eng. vol. 8 (49) (2020) 18062–18070.
[39] M. Pérez-Fortes, J.C. Schöneberger, A. Boulamanti, E. Tzimas, Methanol synthesis using captured CO_2 as raw material: techno-economic and environmental assessment, Appl. Energy vol. 161 (2016) 718–732.
[40] G. Manzolini, A. Giuffrida, P.D. Cobden, H.A.J. van Dijk, F. Ruggeri, F. Consonni, Techno-economic assessment of SEWGS technology when applied to integrated steel-plant for CO_2 emission mitigation, Int. J. Greenh. Gas. Control vol. 94 (February 2019) (2020), 102935.
[41] S. Simoes et al., The JRC-EU-TIMES model. Assessing the long-term role of the SET Plan Energy technologies, Scientific and Policy Report by the Joint Research Center of the European Commision., 2014.
[42] F. Dalena, A. Senatore, A. Marino, A. Gordano, M. Basile, A. Basile, Methanol production and applications: an overview, Elsevier B.V, 2018.
[43] International Organization for Standardization (ISO), Petroleum products - Fuels (class F) - Specifications of dimethyl ether (DME) - ISO 16861." 2015. [Online]. Available: ⟨https://www.iso.org/standard/57835.html⟩.
[44] "KNMI. Normale waarden temperatuur - langjarig gemiddelde 1991–2020, 2021.
[45] Chris Winkelman and Niels Muller, Pricing NL taxation Energy transition, carbon Webcast series 'State of Tax.'"
[46] J.F. Portha, et al., Kinetics of methanol synthesis from carbon dioxide hydrogenation over copper-zinc oxide catalysts, Ind. Eng. Chem. Res. vol. 56 (45) (2017) 13133–13145.
[47] C. Ortega, M. Rezaei, V. Hessel, G. Kolb, Methanol to dimethyl ether conversion over a ZSM-5 catalyst: intrinsic kinetic study on an external recycle reactor, Chem. Eng. J. vol. 347 (August 2017) (2018) 741–753.
[48] S. Poto, J.G.H. Endepoel, M.A. Llosa-Tanco, D.A. Pacheco-Tanaka, F. Gallucci, M. F. Neira d'Angelo, Vapor/gas separation through carbon molecular sieve membranes: experimental and theoretical investigation, Int. J. Hydrog. Energy vol. 47 (21) (2022) 11385–11401.
[49] J.A. Medrano, M.A. Llosa-Tanco, D.A. Pacheco-Tanaka, F. Gallucci, Transport mechanism and modeling of microporous carbon membranes, Elsevier Inc, 2019.
[50] N. Diban, A.M. Urtiaga, I. Ortiz, J. Ereña, J. Bilbao, A.T. Aguayo, Influence of the membrane properties on the catalytic production of dimethyl ether with in situ water removal for the successful capture of co 2, Chem. Eng. J. vol. 234 (2013) 140–148.
[51] R. Mukherjee, Effectively design shell-and-tube heat exchangers, Chem. Eng. Prog. (February) (1998).
[52] T. Barletta, J. Nigg, S. Ruoss, J. Mayfield, W. Landry, Reprinted from: Diagnose flooding Using field pressure data, a refiner made a low-capital modification on a, no. JULY, 2001.
[53] L. March, Introduction to Pinch Technology, 1998.
[54] V. Spallina, et al., Techno-economic assessment of di ff erent routes for ole fi ns production through the oxidative coupling of methane (OCM): advances in benchmark technologies, Energy Convers. Manag. vol. 154 (September) (2017) 244–261.
[55] C.E. Baukal, Industrial Combustion Testing. 2010.
[56] R.S.G. Towler, Chapter 7 - capital cost estimating. Chemical Engineering Design, second ed., Butterworth-Heinemann,, Ed. Boston, 2013, pp. 307–354.
[57] J.R. Couper, Process Engineering Economics. University of Arkansas, Fayetteville, Arkansas (USA), 2003.
[58] T.R. Brown, Capital cost estimating, vol. 79, no. 10. 2000.
[59] R. G. and K. M. N. Warren D. Seider, Daniel R. Lewin, J. D. Seader, Soemantry Widagdo, Product and Process Design Principles - Synthesis, Analysis and Evaluation, 4th editio. 2016.
[60] R. Smith, Chem. Process Des. Integr. Vol. 68 (2005).
[61] M. Nordio, S.A. Wassie, M. Van Sint Annaland, D.A. Pacheco Tanaka, J.L. Viviente Sole, F. Gallucci, Techno-economic evaluation on a hybrid technology for low hydrogen concentration separation and purification from natural gas grid, Int. J. Hydrog. Energy vol. 46 (45) (2021) 23417–23435.
[62] H. Groenemans, G. Saur, C. Mittelsteadt, J. Lattimer, H. Xu, Techno-economic analysis of offshore wind PEM water electrolysis for H2 production, Curr. Opin. Chem. Eng. vol. 37 (2022), 100828.
[63] "Statista. Industrial prices for electricity in the Netherlands 1995–2020, 2021.
[64] "Methanex Monthly Average Regional Posed COntract Price Hystory, 2021. [Online]. Available: ⟨https://www.methanex.com/our-business/pricing⟩.

[65] "PayScale: Chemical Operator Salary in the Netherlands." ⟨https://www.payscale.com/research/NL/Job=Chemical_Operator/Salary⟩.
[66] F. Mac., 30-Year Fixed-Rate Mortgages Since 1971."
[67] C. Brencio, M. Maruzzi, G. Manzolini, F. Gallucci, Butadiene production in membrane reactors: a techno-economic analysis, Int. J. Hydrog. Energy vol. 47 (50) (2022) 21375–21390.
[68] "European Environment Agency. Greenhouse gas emission intensity of electricity generation."
[69] Fortune Business Insight, Dimethyl Ether Market Size, Share & COVID-19 Impact Analysis, by application (LPG blending, aerosol propellant, transportation fuel and others), and regional forecast, 2021–2028, 2021.
[70] A. Trattner, M. Klell, F. Radner, Sustainable hydrogen society – vision, findings and development of a hydrogen economy using the example of Austria, Int. J. Hydrog. Energy vol. 47 (4) (2022) 2059–2079.
[71] IEA, Energy policy review - The Netherlands 2020. Technical report."
[72] R.J. Detz, J.N.H. Reek, B.C.C. Van Der Zwaan, The future of solar fuels: when could they become competitive? Energy Environ. Sci. vol. 11 (7) (2018) 1653–1669.
[73] "IEA CHG Technical report. Economic Evaluation of SMR based standalone (Merchant) hydrogen plant with CCS."
[74] K. Schoots, F. Ferioli, G.J. Kramer, B.C.C. van der Zwaan, Learning curves for hydrogen production technology: an assessment of observed cost reductions, Int. J. Hydrog. Energy vol. 33 (11) (2008) 2630–2645.
[75] M. De Falco, M. Capocelli, A. Basile, Selective membrane application for the industrial one-step DME production process fed by CO_2 rich streams: modeling and simulation, Int. J. Hydrog. Energy vol. 42 (10) (2017) 6771–6786.
[76] P. Pérez-Uriarte, A. Ateka, M. Gamero, A.T. Aguayo, J. Bilbao, Effect of the operating conditions in the transformation of DME to olefins over a HZSM-5 zeolite catalyst, Ind. Eng. Chem. Res. vol. 55 (23) (2016) 6569–6578.
[77] IFRS financial reporting and analysis software., Gross margin-breakdown by industry., 2020.
[78] Elke Asen, Carbon Tax in Europe, 2021.
[79] S. Shiva Kumar, V. Himabindu, Hydrogen production by PEM water electrolysis – a review, Mater. Sci. Energy Technol. vol. 2 (3) (2019) 442–454.
[80] L. Bernadet, G. Gousseau, A. Chatroux, J. Laurencin, F. Mauvy, M. Reytier, Influence of pressure on solid oxide electrolysis cells investigated by experimental and modeling approach, Int. J. Hydrog. Energy vol. 40 (38) (2015) 12918–12928.
[81] P.T. Chang, Q.H. Ng, A.L. Ahmad, S.C. Low, A critical review on the techno-economic analysis of membrane gas absorption for CO_2 capture, Chem. Eng. Commun. vol. 209 (11) (2022) 1553–1569.